Two Related but Distinct Chondroitin Sulfate Mimetope Octasaccharide Sequences Recognized by Monoclonal Antibody WF6*

Peraphan Pothacharoen[‡1], Kittiwan Kalayanamitra[‡§1], Sarama S. Deepa[§], Shigeyuki Fukui[¶], Tomohide Hattori[#], Nobuhiro Fukushima[#], Timothy Hardingham[※], Prachya Kongtawelert[‡2], and Kazuyuki Sugahara[§†3]

[‡]Thailand Excellence Center for Tissue Engineering, Department of Biochemistry, Faculty of Medicine, Chiang Mai University, Chiang Mai 50200, Thailand, [§]Department of Biochemistry, Kobe Pharmaceutical University, Higashinada-ku, Kobe 658-8558, Japan, [¶]Department of Biotechnology, Faculty of Engineering, Kyoto Sangyo University, Kyoto 603-8558, Japan, [#]Science & Technology Systems, Inc. 1-20-1 Shibuya, Shibuya-ku, Tokyo 150-0002, Japan, [※]UK Centre for Tissue Engineering and Wellcome Trust Centre for Cell-Matrix Research, Faculty of Life Sciences, University of Manchester, Manchester M13 9PT, UK, [†]Laboratory of Proteoglycan Signaling and Therapeutics, Frontier Research Center for Post-Genomic Science and Technology, Hokkaido University Graduate School of Life Science, Sapporo, Hokkaido 001-0021, Japan

Running title: structure determination of anti-CS antibody epitopes
Key words: chondroitin sulfate/ epitope/ monoclonal antibody/ octasaccharides/ sulfation/ molecular modeling

ABSTRACT

Chondroitin sulfate (CS) proteoglycans are major components of cartilage and other connective tissues. The monoclonal antibody (mAb) WF6, developed against embryonic shark cartilage CS, recognizes an epitope in CS chains, which is expressed in ovarian cancer and variably in joint diseases. To elucidate the structure of the epitope, we isolated oligosaccharide fractions from a partial chondroitinase ABC digest of shark cartilage CS-C and established their chain length, disaccharide composition, sulfate content and sulfation pattern. These structurally defined oligosaccharide fractions were characterized for binding to WF6 by enzyme-linked immunosorbent assay using an oligosaccharide microarray prepared with CS oligosaccharides derivatized with a fluorescent aminolipid. The lowest molecular weight fraction recognized by WF6 contained octasaccharides, which were split into five subfractions. The most reactive subfraction contained several distinct octasaccharide sequences. Two octasaccharides, **ΔD-C-C-C and ΔC-C-A-D, were recognized by WF6, but other related octasaccharides, ΔC-A-D-C and ΔC-C-C-C, were not. The structure and sequences of both the binding and non-binding octasaccharides were compared by computer modeling, which revealed a remarkable similarity between the shape and distribution of the electrostatic potential in the two different octasaccharide sequences that bound to WF6 and which differed from the non-binding octasaccharides. The strong similarity in structure predicted for the two binding CS octasaccharides (ΔD-C-C-C and ΔC-C-A-D) provided a possible explanation for their similar affinity for the WF6, although they differed in sequence and thus form two specific mimetopes for the antibody.

****Abbreviations:**
A, GlcUAβ1-3GalNAc(4-*O*-sulfate);
C, GlcUAβ1-3GalNAc(6-*O*-sulfate);
D, GlcUA(2-*O*-sulfate)β1-3GalNAc(6-*O*-sulfate);
ΔC, $\Delta^{4,5}$HexUAα1-3GalNAc(6-*O*-sulfate);
ΔD,
$\Delta^{4,5}$HexUA(2-*O*-sulfate)α1-3GalNAc(6-*O*-sulfate).

INTRODUCTION

Chondroitin sulfate proteoglycans (CS-PGs)[4] are expressed on the surface of most cells and in extracellular matrices in vertebrates, where CS is linked to a wide range of core protein families. They are increasingly implicated as important regulators of many biological processes contributing in various ways to the physical strength of tissues, cell adhesion and signal transduction (1-4).

CS chains have a considerable structural variability, the biological functions of which are not well understood. The structure is an unbranched polymer linked through a unique tetrasaccharide (GlcUA-Gal-Gal-Xyl) to a serine residue in a PG, and is composed of repeating disaccharides (-4GlcUAβ1-3GalNAcβ1-)n, which can be modified by *O*-sulfation reactions at various positions, where GlcUA and GalNAc represent D-glucuronic acid and *N*-acetyl-D-galactosamine, respectively. CS is expressed in tissue- and cell-specific forms generated by varying patterns of sulfation, epimerization and chain length, which may account for some of the functional diversity and specificity of PGs to which they are attached. The sulfation pattern of CS varies with aging in cartilage (5). CS-D and CS-E, which contain specific disulfated disaccharide units, promote the neurite outgrowth of hippocampal and

mesencephalic neurons (4, 6, 7). CS sequences are also involved in chemokine binding (8). Sulfation is closely related to key steps in biosynthesis including chain elongation and termination (9).

Monoclonal antibodies (mAbs) have been generated that recognize specific features of CS chains (10), but few of the epitopes have been characterized in detail (11-13). Studies with anti-CS mAbs have revealed restricted spatio-temporal patterns of expression in various tissues during growth and development and in pathological conditions (14-17). The use of antibodies that recognize epitopes on CS chains is becoming more widely used in many fields of biomedical research, such as tissue growth and development (16) and also in the diagnosis of diseases (18-20).

Studies of experimental canine osteoarthritis (OA) cartilage revealed that early in diseases there were distinctive changes in the CS epitopes long before there was any cartilage destruction (20). Changes in the sulfation of CS were also reported in the PG fragments found in synovial fluid following joint trauma (21). Measuring CS epitopes in cartilage metabolites in body fluids of patients with arthritis (22-24) therefore has potential for monitoring the progression and severity of the disease.

WF6 is a mouse IgM type mAb with κ-chains, generated using embryonic shark cartilage CS-PGs as immunogen. It is reactive with shark CS-PGs and the epitope was also detected in commercial CS preparations (CS-C and CS-D) from shark cartilage, but the antibody is unreactive with other glycosaminoglycans (GAGs) (25). Enzyme-linked immunosorbent assay (ELISA) has shown that this mAb detected increased level of WF6 epitope in serum samples from patients of OA and rheumatoid arthritis (RA) (19) and in those of ovarian cancer (20). The established specificity of the antibody and its restricted distribution amongst CS chains has suggested that the epitope is a specific sequence found in some, but not all CS chains, and is composed of sulfated disaccharides including A unit [GlcUAβ1-3GalNAc(4-*O*-sulfate)], C unit [GlcUAβ1-3GalNAc(6-*O*-sulfate)], and D unit [GlcUA(2-*O*-sulfate)β1-3GalNAc(6-*O*-sulfate)]. It was thus important to determine its structure and to understand if such sequences have specific biological functions, as in the case of those recognized by other anti-CS mAbs including CS-56 and MO-225 (11) as well as anti-dermatan sulfate mAb 2A12 (12).

Several studies have investigated the structure of CS chains on PGs from various tissues, but comprehensive methods to determine sulfation sequences do not exist. Progress has therefore been made using mAbs directed to CS (26-29). The epitopes recognized by such mAbs are either sequences containing sulfated disaccharides in native CS chains (14, 30, 31) or unnatural structures with non-reducing terminal unsaturated uronic acid in the chains, which are created by digestion with chondroitinase ABC (32). The mAb WF6, which recognizes a native epitope on CS chains (25), has been found useful in investigating changes in pathological conditions. These results have provided evidence that the expression of the WF6 epitope within CS-PGs is regulated and therefore the generation of such sequences is not a consequence of random sulfation. Characterization of the epitope is thus essential to understand the biological function of these specific chain sequences and the processes that regulate their expression.

To define the key structural features of the CS that are recognized by the mAb WF6, we have isolated and characterized a range of variously sized oligosaccharide fragments from CS-C of shark cartilage and successfully defined two mimetope octasaccharide sequences that are recognized by the mAb. Furthermore, these octasaccharides were analyzed by computer modeling and simulation to reveal their common structural features. Previously the effectiveness of molecular modeling was shown (13). The most stable and the second best stable conformations of the CS octasaccharides recognized by mAbs CS-56, MO-225 and 473HD were very similar with subtle energy difference, and were in good agreement with the structure determined by NMR spectroscopy. However, the accuracy of the used geometry optimization at a classical mechanics level is not sufficient for predicting intermolecular interaction zones because charge values are fixed even when a conformation change is brought about. Therefore, in this study, intrinsic properties of the octasaccharides recognized by mAb WF6 were analyzed at a quantum mechanics level, which gives much more accurate information. The stable structures sampled and optimized adequately by energy minimizations in force field calculations were used as the initial structures in the semi-empirical molecular orbital calculations to solve the electronic structure. Thus, we could derive the intermolecular interaction zones and ESP charges caused by the zones, and reveal the critical zones in the octasaccharide sequences. Comparison of the ESP charges and zones of the preferred and non-preferred octasaccharides successfully demonstrated the common interaction zones and predicted the molecular recognition mechanisms.

EXPERIMENTAL PROCEDURES

Materials-CS-C from shark cartilage and chondroitinase ABC (EC 4.2.2.4) from *Proteus vulgaris* were purchased from Sigma-Aldrich (St. Louis, MO). 6-*O*-Sulfatase or 4-*O*-sulfatase were purchased from Seikagaku Co. (Tokyo, Japan). Bio-Gel P6 was from Bio-Rad (Redmond, CA). Other chemicals were purchased from Sigma-Aldrich, Merck (Dermstadt, Germany), or Boehringer Ingelheim Bioproducts (Heidelberg, Germany) unless specified otherwise. The mAb WF6, which was

produced using embryonic shark cartilage CS-PGs as immunogen in mice (25), is an IgM mAb with κ-light-chain and is reactive with the CS-PG in the A_1D_1 fraction, derived from shark cartilage ($S\text{-}A_1D_1$)(25). Horseradish peroxidase (HRP) conjugated with the secondary antibody against mouse IgM was obtained from Sigma-Aldrich. Shark cartilage CS-antigens A_1 and A_1D_1 fractions were prepared and purified as previously reported (33).

Preparation and Fractionation of CS Oligosaccharide Fragments-The commercial CS-C preparation from shark cartilage was partially depolymerized by controlled digestion with chondroitinase ABC. In brief, 1 g of CS-C was digested with 5 units of the enzyme in 5 ml of 0.05 M Tris-HCl, pH 8.0, containing 0.06 M CH_3COONa at 37 ^oC overnight. The digest was desalted on a short column of Sephadex G-10 and fractionated on a column (1.6 x 100 cm) of Bio-Gel P-6 in 0.2 M ammonium acetate at a flow rate 15 ml/h. The lowest molecular weight fraction (fraction C6), which competed with the binding of WF6, was subfractionated on a short MonoQ FPLC cartridge column (5 ml) of strong anion exchange resin (SAX) (Amersham Biosciences, Tokyo, Japan) with detection at 232 nm. The yield of fraction C6 from 1 g of CS-C was 13 mg, and a portion (11 mg) was used for the purification. Elution was carried out using a linear gradient of $LiClO_4$ from 0 to 0.25 M over 30 min at a flow rate of 1 ml/min. One ml fractions were collected. The subfractions were desalted on a short PD-10 column of Sephadex G-25 (Amersham Biosciences) and lyophilized. Determination of the molecular mass of the oligosaccharide in each subfraction was carried out by MALDI-TOF MS, and quantitation was made by the carbazole reaction for uronic acid using GlcUA as a standard (34).

Delayed Extraction Matrix-assisted Laser Desorption Ionization Time-of-flight Mass Spectrometry (DE MALDI-TOF/MS)-DE MALDI-TOF/MS of oligosaccharide fractions were acquired in a Voyager DE-RP/Pro (PerSeptive Biosystems, Framingham, MA) in a linear mode. Gentisic acid (Sigma-Aldrich) was used as the matrix at a concentration of 1 mg/ml in water. A synthetic peptide $(Arg\text{-}Gly)_{15}$ was used as a complexing agent to shield the negatively charged groups of the sulfated oligosaccharides (35). An aqueous solution of $(Arg\text{-}Gly)_{15}$ (10 pmol/μl) was first mixed with 10 pmol of each oligosaccharide fraction and then with 1 μl of the matrix solution. The mixture was placed on the probe surface, dried under a stream of air and used for the measurement of the spectrum.

Derivatization of Reducing Oligosaccharides with 2-Aminobenzamide-The derivatization of oligosaccharides with a fluorophore 2-aminobenzamide (2AB) was performed essentially as described by Bigge *et al*. (36). Briefly, 0.1- 0.5 nmol of a given oligosaccharide was lyophilized in a microcentrifuge tube. An aliquot (5 μl) of a derivatization reagent solution (0.35 M 2AB/0.1 M $NaCNBH_4$/30% (v/v) acetic acid in dimethyl sulfoxide) was added to the oligosaccharide sample, and the mixture was incubated at 65 ^oC for 2 h. The derivatized oligosaccharide was purified by paper chromatography using Whatman 3 MM paper in a solvent system of butanol:ethanol:water (4:1:1, v/v/v).

HPLC-The fractionation and analysis of unsaturated oligosaccharides were performed by anion-exchange HPLC on an amine-bound silica PA-03 column with a linear gradient of NaH_2PO_4 at a flow rate of 1 ml/min at room temperature as described for the separation of CS disaccharides and tetrasaccharides (37). Eluates were monitored using an RF-10A_{XL} fluorometric detector (Shimadzu Co., Kyoto, Japan) with excitation and emission wavelengths of 330 and 420 nm, respectively. Unsaturated oligosaccharides (0.3 to 1.0 nmol aliquots) unlabeled with 2AB were monitored by absorbance at 232 nm.

Strategy for Exo-sequencing of CS-C Octasaccharide-Each octasaccharide fraction (30 picomoles) was derivatized with 2AB. The excess 2AB reagent was removed by paper chromatography and an aliquot (5 picomoles) of the 2AB derivatized octasaccharide fraction was digested with chondroitinase ABC or AC-II, and analyzed by anion-exchange HPLC on an amine-bound silica column to identify the disaccharide units to be released from the reducing side (Step one). Another digest (5 picomoles) with chondroitinase ABC or AC-II of each digest was labeled with 2AB again, purified by paper chromatography, and analyzed by anion-exchange HPLC to identify the disaccharide units to be released from the non-reducing end and the penultimate position of the octasaccharide (See Scheme 1).

Competitive ELISA for WF6-Purified shark aggrecan aggregate (A_1-fraction) was absorbed overnight on a polystyrene Maxisorp® plate (Nunc, Roskilde, Denmark) at 10 μg/ml in 0.2 M $NaHCO_3$, pH 9.6 in 100 μL per well at room temperature. The wells were washed 3 times with 0.2 M Tris-HCl buffer, pH 7.4 and blocked with 1% (w/v) bovine serum albumin (BSA) in the Tris buffer for 1 h at 37 ^oC. The coated wells were incubated with a mixture of mAb WF6 (1:20,000) with a standard (the A_1D_1 fraction of shark cartilage aggrecan) or a sample in blocking reagent for 1 h at 37 ^oC. For competition studies, mAb WF6 was preincubated with different GAGs (CS polysaccharide or oligosaccharide) for 1 h at 37 ^oC at various concentrations (see results) and added to the immobilized the A_1 fraction in the presence of

soluble competitors. The plates were washed 3 times with the Tris buffer and incubated for 1 h at 37 ^{o}C with specific anti-mouse IgM (μ-chain) secondary antibodies coupled with HRP diluted 2,000-fold in the Tris buffer. After washing 3 times, the plates were developed with *ortho*-phenylenediamine (Sigma Aldrich). The colored reaction product was quantified in an ELISA reader Titertek Multiscan (Flow Laboratories, Mecklenheim, Germany) by absorbance OD at 452 nm. Experiments were performed in duplicate. The percent inhibition was calculated as follows: % inhibition= 100 – [([OD_{test} – OD_{blank}]/ [$OD_{control}$-OD_{blank}]) x 100].

Derivatization of CS-derived Oligosaccharide with Fluorescent Aminolipid-CS-C oligosaccharides were coupled to *N*-aminoacetyl-*N*-(9-anthracenylmethyl)-1,2-dihexadecyl-sn-glycero-3-phosphoethanolamine (ADHP), synthesized from anthracenaldehyde and 1,2-dihexadecyl-*sn*-glycero-3-phosphoethanolamine, gives an intense fluorescence under UV light as described previously (38). Briefly, a dried oligosaccharide fraction (2 nmol as oligosaccharide) was mixed with 6 nmol ADHP in chloroform/methanol/water, 10:10:1 (v/v/v). The reaction mixture was sonicated in a bath, heated at 60 ^{o}C for 2 h. Tetrabutylammonium cyanoborohydride (100 nmol in 2 μl of methanol) was added, and after sonication for 5 min, the mixture was incubated at 60 ^{o}C for 72 h. The reaction mixture was dried in a vacuum concentrator, and dissolved in chloroform/methanol/water 25:25:8 (v/v/v), and purified by thin layer chromatography in a solvent system of chloroform/methanol/0.2 M $CaCl_2$ (105:10:28, v/v/v) for oligosaccharide microarray analysis.

CS Oligosaccharide Microarrays-The preparation of CS-C oligosaccharide microarrays was carried out as described previously (38) with slight modifications. Briefly, CS-C oligosaccharides derivatized with the fluorescent lipid were dissolved in chloroform/methanol/0.2 M $CaCl_2$ (105:10:28, v/v/v), and applied onto a 0.45 μm nitrocellulose membrane (Bio-Rad) as 2 mm-width bands by jet spray using a sample applicator (Linomat V, Camag, Switzerland) at a spotting rate of 70 nl/sec. Each membrane was blocked with 3% (w/v) BSA in PBS, pH 7.4 for 1 h and overlaid with mouse IgM mAb WF6 diluted 500-fold) in 3% (w/v) BSA in PBS, pH 7.4 for 2 h. The membranes were rinsed several times with 3% (w/v) BSA in PBS, pH 7.4 and overlaid for 1 h with anti-mouse IgM conjugated with HRP diluted 3,000-fold with 3% (w/v) BSA in PBS, pH 7.4. The binding of the antibody was visualized using FAST 3,3'-diaminobenzidine (DAB-FAST, Sigma Aldrich) according to the manufacturer's instruction.

Determination of Uronic Acid-GlcUA was determined with a colorimetric assay using the carbazole reaction (34) with GlcUA as a standard. Unsaturated uronic acid was quantified spectrophotometrically based on an average millimolar absorption cofficient of 5.5 at 232 nm (40).

Analysis of the Dihedral Angles of CS Disaccharides determined at the Local Energy Minima-The dihedral angles (ϕ, ψ) of a given CS disaccharide largely determine its conformation. The dihedral angles (ϕ, ψ) of the local energy minima were calculated for the five disaccharide subunits included in the above octasaccharides: [GlcUAβ1-3GalNAc(4-*O*-sulfate), GlcUAβ1-3GalNAc(6-*O*-sulfate), GlcUA(2-*O*-sulfate)β1-3GalNAc(6-*O*-sulfate), GalNAc(4-*O*-sulfate)β1-4GlcUA(2-*O*-sulfate), and GalNAc(6-*O*-sulfate)β1-4GlcUA]. The previous study (13) had demonstrated that eight CS disaccharide subunits had local energy minimum conformations with roughly similar (ϕ, ψ) values around (80°, 100°), (300°, 100°), (80°, 300°), and (300°, 300°) in each adiabatic map (13). In this study, to obtain the (ϕ, ψ) values of the local minimum conformations of the above disaccharides, the twenty-four conformations in each disaccharide in the range of (40°-330°, 60°-330°) were chosen and full geometry optimizations were performed using the semi-empirical molecular orbital calculations with the Accelrys Materials Studio's module (URL: http://www.accelrys.com/products/mstudio/) taking the solvent effects into consideration. Likewise, the dihedral angles of the disaccharide constituents of the other CS octasaccharides were determined.

Molecular Modeling and Computational Analyses-Molecular dynamics and semi-empirical molecular orbital calculations were performed to explain the biological activity of the four isolated oligosaccharides (ΔC-A-D-C, ΔC-C-C-C, ΔC-C-A-D and ΔD-C-C-C). Their geometries were constructed using the Accelrys Materials Studio's module (URL: http://www.accelrys.com/products/mstudio/), and their equilibrium structures were optimized by the anneal dynamics consisting of a dynamics simulation, where the temperature was periodically increased from an initial temperature to a mid-cycle temperature and back again to the initial temperature using the Forcite module (41, 42). The anneal dynamics optimizations were performed with the temperature ramped from 300 to 500 K and the annealing of 20 cycles using the Forcite universal force field (41, 42). The equilibrium structures derived from the anneal dynamics were used as the starting structure in semi-empirical molecular orbital calculations. All self-consistent field calculations were converged to a root-mean-square change in the density change of less than 1.0 x 10^{-5} hartree utilizing

the semi-empirical HF AM1 Hamiltonian and the solvent effect modeled using the COnductor-like Screening MOdel (COSMO) (43, 44) with the dielectric constant of 78.54 (water solvation). Full geometry optimizations were converged to a root-mean-square change in the force change of less than 1.0 kcal/mol/ Å using the VAMP module (45-51). The optimized structure of the ΔD-C-C-C octasaccharide was also used as a template for determination of the molecular superimposition. The root mean square deviation (RMSD) was the measure of the average distance between the backbones of superimposed oligosaccharides. The ESP distribution based on the Natural Atomic Orbital Point Charge (NAO-PC) model (52) was calculated using the HF AM1 semi-empirical molecular orbital method and was fitted with the atomic point charges.

RESULTS

The WF6 Epitope Is Present in the CS Chains of Aggrecan Isolated from Shark Cartilage-The specificity of mAbWF6 was tested by competitive ELISA with CS-PGs from shark cartilage as antigen. Commercial preparations of CS-C containing predominantly C disaccharide unit [GlcUA-GalNAc(6-*O*-sulfate)] and CS-D characterized by D unit [GlcUA(2-*O*-sulfate)-GalNAc(6-*O*-sulfate)] gave 50% inhibition at 100 and 1.1 μg/ml, respectively. Other GAGs including CS-A rich in A unit [GlcUA-GalNAc(4-*O*-sulfate)], CS-E rich in E unit [GlcUA-GalNAc(4, 6-*O*-disulfate)], dermatan sulfate rich in iA unit [iduronic acid-GalNAc(4-*O*-sulfate)] (53), hyaluronan and keratan sulfate showed no significant inhibitory activity. Aggrecan-related CS-PGs such as the shark cartilage A_1D_1 fraction ($S\text{-}A_1D_1$) showed 50% inhibition at 0.60 μg/ml, whereas no significant inhibition was observed with the aggrecan core protein (chondroitinase ABC-digested aggrecan from porcine laryngeal cartilage). Thus, the results confirmed that WF6 reacted with CS from different sources and suggested that the specificity was for a sub-set of CS chains. The reactivity was noted to be strongest with CS-D chains rich in "D" disaccharide units.

Fragmentation of CS-C and the Evaluation of the Reactivity of the CS Oligosaccharides with the mAb WF6-A partial digest of a commercial CS-C preparation (1 g) with chondroitinase ABC (Fig. 1) was fractionated by gel filtration on a column of Bio-Gel P-6 into subfractions (C1-C9), which were tested using samples containing up to 200 μg of uronic acid for inhibition of the binding of mAb WF6 to immobilized CS-PG aggregate from shark cartilage (A_1 fraction). At low concentrations (samples containing 100 and 50 μg uronic acid), the subfractions C1-C6 showed considerable inhibitory activity, whereas fractions with smaller hydrodynamic sizes than fraction C6 (C7-C9) showed only weak inhibitory activity (Fig. 1B). Thus, the inhibitory activity of the subfractions decreased with chain length. Based on these results, fraction (C6) was subfractionated by strong anion-exchange (SAX) chromatography on a MonoQ column (Fig. 2A), and five major subfractions (C6A-C6E) were obtained by rechromatogarphy under the same conditions (Table I). The yield of these fractions is summarized in Table I. When the inhibitory activity was compared amongst the SAX subfractions (tested at 200 μg uronic acid per sample), C6C gave the strongest inhibition (75%) at 200 μg, whereas C6D and C6E were less inhibitory (33 and 58%, respectively) (Fig. 2B). The direct binding to mAb WF6 was determined with an oligosaccharide microarray using the ADHP-labeled oligosaccharides. Only fraction C6E showed direct binding (Fig. 2C), suggesting that the mAb epitope was present only in fraction C6E but not in C6A, C6B, C6C or C6D.

Characterization of the Oligosaccharides in the SAX Subfractions-The SAX-subfractions (C6A-C6E in Fig. 2A) were labeled with a fluorophore 2AB for sensitive detection, and their purity was examined by anion-exchange HPLC on an amine-bound silica PA-03 column (data not shown), which showed 50-80% purity of these fractions (Table I). The SAX subfractions were also analyzed by MALDI-TOF MS, which showed that fractions C6C, C6D and C6E contained octasaccharides with four to six sulfate groups (Table II), whereas fractions C6A and C6B gave no signal for reasons unknown. The molecular mass of the major compound in fraction C6E was calculated to be 1,934 and 1,954 by subtracting the *m/z* value of the protonated peptide (*m/z* 3,213.98) from that of the protonated peptide/oligosaccharide complex (m/z 5,142.27 and 5,223.88); this corresponded to a pentasulfated octasaccharide and a hexasulfated octasaccharide, respectively (Table II). The results revealed that fraction C6C contained predominantly tetrasulfated octasaccarides, whereas fractions C6D and C6E were a mixture of tetra- and pentasulfated octasaccharides and a mixture of penta- and hexasaulfated octasaccharides, respectively. Disaccharide composition analysis of the fractions C6A - C6E was also carried out after digestion with chondroitinase ABC and subsequent labeling with 2AB followed by anion-exchange HPLC on an amine-bound silica column. The results suggested that the major components in fractions C6B to C6D are composed mainly of C/ΔC and minor A/ΔA disaccharide units, whereas the major component in fraction C6E was most likely pentasaulfated octasaccharide containing two C/ΔC units and one unit each of A or ΔA and D or ΔD disaccharide unit (Table I). Since these fractions still were not homogeneous, fractions C6C, C6D and C6E, which showed the strong inhibitory activity against the binding of the mAb WF6 to the CS-PGs, were

subjected to anion-exchange HPLC for further purification below.

Extensive Purification and Enzymatic Characterization of the Major Octasaccharide Subfractions C6C-C6E-The C6C-C6E SAX-subfractions were further purified by anion-exchange HPLC on an amine-bound silica column. As shown in Fig. 3A and B, fractions C6C and C6D yielded a major component C6Cp1 and C6Dp1, respectively, which were eluted at the same position, whereas fraction C6E gave three subfractions C6Ep1, C6Ep2 and C6Ep3. The major oligosaccharide in each fraction was characterized to reveal the yield, purity and the disaccharide composition (Table III). All fractions except C6Ep2 were found to be more than 95% pure, and they were subjected to sequencing and assays for their reactivity to the mAb WF6 as described below.

Sequencing of the Purified Oligosaccharides—The sequencing of the major oligosaccharides in the isolated fractions was achieved by the strategy illustrated in Scheme 1 according to the method, which has been successfully applied to the sequencing of CS hexa- (37) and octasaccharides (54-56). Upon disaccharide composition analysis fractions C6Cp1 and C6Dp1 yielded only ΔC, suggesting that the major octasaccharide in both the fractions was ΔC-C-C-C. This may have resulted from poor separation of a minor C6D fraction from the major C6C fraction (Fig. 2A). The sequencing of the major component in fraction C6Ep2 is described below in detail with additional relevant information for fractions C6Ep1 and C6Ep3.

Sequencing of the Major Oligosaccharide in Fraction C6Ep2—Disaccharide composition analysis of fraction C6Ep2 was first performed after digestion with chondroitinase ABC. The released disaccharides were labeled with 2AB and analyzed by anion-exchange HPLC on an amine-bound silica column, which yielded 2AB-labeled ΔC [ΔHexUA-GalNAc(6S)], ΔA [ΔHexUA-GalNAc(4S)] and ΔD [ΔHexUA(2S)-GalNAc(6S)] as major components in a molar ratio of 2.04 : 0.78 : 1.00 (Table III), which was consistent with the results obtained by MALDI-TOF MS analysis. These results indicated that the major component in fraction C6Ep2 was composed of two C-units and one unit each of A and D with one of the four units being unsaturated at the non-reducing terminal.

To determine the sequence of these disaccharides in the octasaccharide fraction, C6Ep2 (30 picomoles) was labeled with 2AB, purified by paper chromatography to remove the derivatizing reagents, and then an aliquot (5 picomoles) of the 2AB-labeled sample was subjected to digestion with chondroitinase AC-II or ABC followed by anion-exchange HPLC (Scheme 1). Based on known enzyme specificity (55, 56), chondroitinase AC-II was predicted to degrade a 2AB-labeled unsaturated octasaccharide into four disaccharides: one 2AB-labeled unsaturated disaccharide unit derived from the reducing terminal and three unlabeled unsaturated disaccharide units derived from the non-reducing terminal and internal positions. In contrast, chondroitinase ABC, which cannot digest a 2AB-labeled tetrasaccharide, was predicted to cleave a 2AB-labeled unsaturated octasaccharide into one 2AB-labeled tetrasaccharide from the reducing terminal and two unsaturated disaccharides from the non-reducing terminal and the internal position (55, 56). Hence, digestion with chondroitinase AC-II was used to reveal the reducing terminal disaccharide unit, while chondroitinase ABC helped identify not only the reducing terminal disaccharide but also the disaccharide adjacent to the reducing terminal disaccharide.

The 2AB-derivatized parent octasaccharide gave a symmetrical peak on HPLC (Fig. 4A), and was completely digested with chondroitinase ABC (Fig. 4B). The resultant 2AB-labeled fragment was eluted at the position of an authentic ΔA-D tetrasaccharide (Fig. 4B), and was co-eluted with the authentic ΔA-D (57) upon co-chromatography (data not shown), suggesting that the tetrasaccharide sequence on the reducing side is A-D. The chondroitinase AC-II digest also yielded the ΔA-D tetrasaccharide (data not shown, Table IV). The results are consistent with the recent finding that chondroitinase AC-II does not cleave a hexosaminidic linkage to a "D" disaccharide unit in CS-C chains (55). Thus, a tetrasaccharide-2AB rather than a disaccharide-2AB was generated from the reducing terminal of the octasaccharide.

To determine the disaccharide units from the non-reducing terminus and the internal position, another portion (5 picomoles) of each digest of 2AB-labeled fraction C6Ep2 was derivatized with 2AB again, and analyzed by anion-exchange HPLC. The results are summarized in Table V. The chondroitinase ABC digest gave a peak of 2AB-labeled ΔC and a peak of a 2AB-derivative of tetrasaccharide (ΔA-D) in a ratio of 2.06 : 1.00 (Fig. 4C), suggesting that both the non-reducing terminal and the penultimate units are ΔC. The chondroitinase AC-II digest also gave similar results (Table V). A small proportion of ΔA detected in both the chondroitinase ABC and AC-II digests was assumed to be derived from a minor contaminant in fraction C6Ep2. Based on all these results, it was concluded that the sequence of the major octasaccharide in fraction C6Ep2 is ΔC-C-A-D [ΔHexUAβ1-3GalNAc(6S)β1-4GlcUAβ1-3GalNAc(6S)β1-4GlcUAβ1-3GalNAc(4S)β1-4GlcUA(2S)β1-3GalNAc(6S)] (Table III).

Sequencing of the Major Oligosaccharide in Fraction C6Ep1—The same strategy was used to sequence the major oligosaccharide in fraction C6Ep1. Disaccharide composition analysis of fraction C6Ep1 showed ΔC and ΔD in a molar ratio of 3.17 : 1.00 (Table III), suggesting that the major component in C6Ep1 was composed of three C-units and one D-unit with one of the four units being unsaturated at the non-reducing end. The 2AB-derivatized C6Ep1 was digested with chondroitinase ABC, and anion-exchange HPLC analysis of the digest revealed a 2AB-tagged ΔC-C as a major tetrasaccharide product (89%) with a minor 2AB-tagged ΔD-C (11%), which was eluted at the position of authentic ΔD-C (55, 58) (Table IV), suggesting the reducing terminal sequence of C-C in the major octasaccharide in C6Ep1. The identity of the disaccharide derived from the non-reducing terminus was determined after derivatizing the digest again with 2AB. Anion-exchange HPLC of the 2AB-labeled chondroitinase ABC digest gave 2AB-derivatives of ΔC, ΔD and ΔC-C in a molar ratio of 0.39 : 1.00 : 1.03, while the 2AB-labeled chondroitinase AC-II digest gave ΔC and ΔD in a molar ratio of 2.50 : 1.00 (Table V). Thus, the results suggested two possible octasaccharide sequences ΔD-C-C-C and ΔC-D-C-C, but did not identify if it was ΔC or ΔD that was located at the non-reducing terminus.

To resolve this question, exo-sequencing of the major oligosaccharide in fraction C6Ep1 was carried out taking advantage of the specificity of the highly purified chondroitinase ABC preparation (see "Experimental Procedures"), which only cleaves disaccharides stepwise from the non-reducing terminal (59). The 2AB-derivative of fraction C6Ep2 was first partially digested with the highly purified enzyme preparation and a part of the digest was analyzed by anion-exchange HPLC, which revealed 2AB-derivatives of the parent octasaccharide (85.0%) and the hexasaccharide (15.0%) (Table IV). The released 2AB-labeled hexasaccharide was identified as 2AB-labeled ΔC-C-C since it co-eluted when chromatographed with authentic 2AB-ΔC-C-C prepared previously (59) or by partial digestion of 2AB-labeled D-C-C-C (55) with chondroitinase ABC, and was eluted approximately 1 min later than authentic C-C-C hexasaccharide (60). To identify the disaccharide derived from the non-reducing terminus, a portion of the digest of 2AB-labeled C6Ep1 was derivatized with 2AB again and the labeled-oligosaccharide mixture was analyzed by anion-exchange HPLC (Table V). The results revealed a peak of 2AB-labeled ΔD (5.9%) together with peaks of 2AB-derivatives of ΔC-C-C (14.4%) and ΔD-C-C-C (79.7%), suggesting that the non-reducing terminal was ΔD. Based on these results, it was concluded that the sequence of the major octasaccharide in fraction C6Ep1 is ΔD-C-C-C [ΔHexUA(2S)α1-3GalNAc(6S)β1-4GlcUAβ1-3GalNAc(6S)β1-4GlcUAβ1-3GalNAc(6S)β1-4GlcUAβ1-3GalNAc(6S)] (Table III).

Sequencing of the Major Oligosaccharide in Fraction C6Ep3—Disaccharide composition analysis of fraction C6Ep1 showed ΔC, ΔA and ΔD in a molar ratio of 2.12 : 1.00 : 0.65 (Table III), suggesting that the major compound in fraction C6Ep3 was composed of two C-units, one each of A-unit and D-unit with one of the four units being unsaturated at the non-reducing end. The 2AB-labeled C6Ep3 was digested with chondroitinase AC-II, and anion-exchange HPLC analysis of the digest revealed 2AB-tagged ΔC as a sole 2AB-labeled product (Table IV), suggesting that the reducing terminal disaccharide is C-unit. Consistent with this result, a chondroitinase ABC digest of the 2AB-derivatized C6Ep3 yielded major 2AB-labeled ΔD-C (88%) with a minor product of 2AB-labeled C-C (12%) derived from a minor octasaccharide in fraction C6Ep3 (Table IV). The results suggest the D-C tetrasaccharide sequence on the reducing side of the major octasaccaride. To examine the disaccharide units at the non-reducing end and the penultimate position, the chondroitinase ABC digest was labeled with 2AB again and analyzed by HPLC, which showed 2AB-derivatives of ΔD-C, ΔC and ΔA in a molar ratio of 1.00 : 1.00 : 0.77. The results suggested two possible sequences ΔA-C-D-C and ΔC-A-D-C as a major octasaccharide, but did not discriminate between the two. Since the latter sequence has been isolated from shark cartilage CS-D (29), it was labeled with 2AB and co-chromatographed with the 2AB-labeled C6Ep3 on anion-exchange HPLC. The major 2AB-labeled component in fraction C6Ep3 was co-eluted with authentic 2AB-labeled ΔC-A-D-C (data not shown). Although ΔA-C-D-C has never been isolated, 2AB-labeled ΔC-A-D-C can most likely be separated and discriminated from 2AB-labeled ΔA-C-D-C in view of the high resolution (Fig. 3) of the related but distinct octasaccharide sequences. Based on these results, it was concluded that the major component in fraction C6Ep3 was ΔC-A-D-C [ΔHexUAα1-3GalNAc(6S)β1-4GlcUAβ1-3GalNAc(4S)β1-4GlcUA(2S)β1-3GalNAc(6S)β1-4GlcUAβ1-3GalNAc(6S)] (Table III).

Reactivity of the mAb WF6 Toward the Purified Fractions Containing Structurally Defined Octasaccharides-Extensive fractionation yielded relatively small amounts of the purified fractions containing the structurally defined CS-C octasaccharides (Table III). It has previously been demonstrated that only one picomole of aminolipid (ADHP) derivatives of CS/DS oligosaccharides, when immobilized on a nitrocellulose membrane for microarray, were sufficient for detection of specific binding of anti-CS antibodies and other

carbohydrate-binding proteins to CS oligosaccharide chains (38). Therefore, the neoglycolipids of the purified fractions C6Ep1 – C6Ep3 were prepared and spotted onto a nitrocellulose membrane in a low picomole range (approx. 2.5 pmol per spot). These lipid derivatives were immobilized on the membrane with similar efficiency, as assessed by the similar fluorescent intensity given by each neoglycolipid spot detected (Fig. 5, upper panel). WF6 reacted preferentially with C6Ep1 and C6Ep2, which contained ΔD-C-C-C and ΔC-C-A-D, respectively, as a major component (Fig. 5, lower panel). Although the two sequences (ΔC-C-A-D) recognized by the mAb have not previously been isolated, octasaccharide fractions containing the corresponding saturated counterpart sequences (D-C-C-C or C-C-A-D) were individually isolated from shark cartilage CS-C in a recent study (55). Hence, the fraction VIIh2.2 containing C-C-A-D was also tested to confirm the reactivity to WF6 (Fig. 5). Although the two preferred sequences shared the C-C tetrasaccharide sequnce, ΔC-C-C-C without D unit was not recognized. It appeared that a rare D disaccharide unit in the two reactive sequences may play a critical role for the recognition by the mAb. However, fraction C6Ep3 containing ΔC-A-D-C was not recognized by the mAb, suggesting the importance of specific sequences, which may share a common conformation. To clarify this point and to exclude a slight possibility that a minor component in each fraction was reactive to the mAB, molecular modeling studies were performed below to analyze the 3D structures or conformations as well as the molecular shapes of the isolated octasaccharide sequences.

Comparison of the Dihedral Angles (ϕ, ψ) in the Five Disaccharide Subunits Included in the Four Isolated Octasaccharides- First of all, the (ϕ, ψ) values of the disaccharides in the local energy minima were determined by full geometry optimizations at the quantum mechanics level (Table VIA). The (ϕ, ψ) values revealed the most stable conformation around (80°, 100°) and (300°, 100°). The maximum difference in the formation energy among the three stable local minimum conformations was 1.2 kcal/mol for GlcUA-GalNAc(6S), 1.1 kcal/mol for GlcUA-GalNAc(4S), 2.9 kcal/mol for GlcUA(2S)-GalNAc(6S), 0.5 kcal/mol for GalNAc(6S)-GlcUA, and 3.5 kcal/mol for GalNAc(4S)-GlcUA(2S). However, the maximum difference in the formation energy among the conformations in the four local energy minima for GlcUA-GalNAc(6S), GlcUA-GalNAc(4S), GlcUA(2S)-GalNAc(6S), GalNAc(6S)-GlcUA, and GalNAc(4S)-GlcUA(2S), was 7.3, 11.8, 7.0, 1.1, and 4.5 kcal/mol, respectively. Therefore, these results suggest that GlcUA-GalNAc(6S), GlcUA-GalNAc(4S), and GlcUA(2S)-GalNAc(6S) may take at least three conformations, whereas GalNAc(6S)-GlcUA and GalNAc(4S)-GlcUA(2S) may take four, because the energy barriers among these local minima are so low. This trend is very similar to that found in the previous study (13) for the stable conformations of the related CS disaccharides, although the range of the dihedral angles obtained in the present study is wider. The (ϕ, ψ) values of the disaccharide constituents in the four octasaccharide sequences were also determined by full geometry optimizations (Table VIB), and showed: (285°±28°, 108°±47°) for GlcUA-GalNAc(6S); (287°±5°, 117°±9°) for GlcUA-GalNAc(4S); (286°±6°, 112°±18°) for GlcUA(2S)-GalNAc(6S); (288°±23°, 237°±30°) and (274°±14°, 73°±27°) for GalNAc(6S)-GlcUA; and (298°±1°, 241°±5°) for GalNAc(4S)-GlcUA(2S). However, a local minimum conformation was not found around the (ϕ, ψ) values of (80°, 300°), where GalNAc(6S)-GlcUA and GalNAc(4S)-GlcUA(2S) showed local minimum conformations in the previous study of the CS disaccharide system (13).

Thus, three or four conformations in the energy local minima were predicted for each CS disaccharide, whereas the full geometry optimization of the octasaccharide sequences identified one or two most stable conformations for the individual disaccharide constituents. These results suggest that the conformation of the CS octasaccharides may be more restricted than that of the individual CS disaccharides. This may be caused by intramolecular interactions among the disaccharide constituents in the octasaccharide sequence. Therefore, the analysis of the conformation of the individual disaccharides is useful, but not sufficient to predict the conformation of larger oligosaccharides composed of the disaccharide units. Therefore, the whole of each octasaccharide sequence was simulated using the potentially more accurate molecular orbital calculation method.

Comparison of the Three-dimensional Structures of the Four Isolated Octasaccharides-The results from the geometry optimizations of the four isolated octasaccharides (ΔC-A-D-C, ΔC-C-C-C, ΔC-C-A-D and ΔD-C-C-C) showed the structures predicted by semi-empirical molecular orbital calculations (Fig. 6). The predicted 3D models of the preferred and non-preferred octasacharides are slightly different. As shown in Fig. 7, the superimposed structures of the predicted structural models showed that the conformations of ΔD-C-C-C and ΔC-C-A-D are dissimilar in spite of the preference by the mAb WF6, but those of ΔD-C-C-C recognized and ΔC-C-C-C, which is not recognized by the mAb, are similar. The calculated RMSD between the backbones of the superimposed octasaccharides was as follows: 4.898 Å for ΔD-C-C-C *vs* ΔC-C-A-D; 4.929 Å for ΔD-C-C-C *vs* ΔC-A-D-C, 4.033 Å for ΔD-C-C-C *vs* ΔC-C-C-C; 0.369 Å for ΔC-C-A-D *vs* ΔC-A-D-C, 6.693 Å for ΔC-C-A-D *vs* ΔC-C-C-C. These results

comparing the simple 3D structures or conformations did not reasonably explain the common recognition of the preferred octasaccharides, ΔD-C-C-C and ΔC-C-A-D, by the mAb WF6. Hence, further analysis was used to compare the ESP distribution for the four isolated octasaccharide sequences to investigate in more detail their molecular shape and charge.

Comparison of the ESP Distribution Maps of the Four Isolated Octasaccharides-The ESP distribution, which influences the recognition by the mAb, was calculated based on the NAO-PC model for the four isolated octasaccharide sequences (52), and is displayed in Fig. 8. The ESP distribution showed the electronegative zones for both the sulfate groups and the carboxy groups having the negative clouds of the oxygen atoms and these zones would interact directly with the mAb. Interestingly, the ESP distribution maps have revealed that the electronegative zones of the preferred octasaccharides (ΔD-C-C-C and ΔC-C-A-D) have similar shapes (Figs. 8A and 8B), but the non-preferred ΔC-C-C-C has a distinct shape (Fig. 8D). Although ΔC-C-A-D, which is recognized by WF6, has a certain similarity to ΔC-A-D-C (Fig. 8C) in terms of the ESP distribution, the electronegative zones of ΔD-C-C-C and ΔC-C-A-D were slightly different from that of ΔC-A-D-C when both ends of these octasaccharides were compared. Another similar feature is that the shapes of the electronegative zones of ΔD-C-C-C and ΔC-C-A-D are spread over the non-reducing terminal of the octasaccharides in contrast to those of ΔC-A-D-C and ΔC-C-C-C. Thus, the comparison of the ESP distribution maps identified the structural features, which were common to the preferred octasaccharides and distinguished them from the non-preferred octasaccharides.

Mulliken and ESP Charges of the Sulfate and Carboxy Groups-The Mulliken population analysis (61) of the charge distributions is the simple and most familiar method to count electrons associated with an atom, and was used for the analysis of the four octasaccharides here. However, nearly constant negative values were obtained for the Mulliken atomic charges of the four carboxy groups in each octasaccharide sequence as shown in Table VIIIA, and did not account for the difference in the molecular recognition by the mAb WF6. Therefore, ESP charge values were calculated. ESP atomic point charges have contributions from both the nuclei and electrons unlike the Mulliken atomic charges, which reflect only the charge distributions (62). For a quantitative analysis of ESP distributions, ESP atomic point charges of sulfate groups and carboxy groups, which make large contributions in the ESP distribution maps. The results are summarized in Tables VII and VIIIB. The polar sulfate groups of both the ΔD unit of ΔD-C-C-C and the ΔC^1 unit of ΔC^1-C^2-A-D showed large negative net charges in each octasaccharide. In ΔD-C-C-C the 2-*O*-sulfate of the ΔD unit had net charges of -1.42. In ΔC^1-C^2-A-D, the value for the 6-*O*-sulfate of the ΔC^1 unit had -1.84 and those for the 2-*O*-sulfate and 6-*O*-sulfate of the D unit were -1.54 and -1.36, respectively. For ΔC-A-D-C, ΔC unit had a smaller negative net charge (-0.87) when compared with those of the non-reducing terminal units of preferred ΔD-C-C-C and ΔC^1-C^2-A-D. The negative net charges of the sulfate groups for ΔC-C-C-C were small (-0.18 ~ -1.17) and diffuse, which reduces the intensity of the electronegative zones and appears to weaken the recognition by the mAb WF6. Thus, these results suggest the involvement of the sulfate groups on both ends of the preferred octasaccharides in the recognition by WF6.

The polar carboxy group of the C^2 unit in ΔD-C^1-C^2-C^3 and that of the D unit in ΔC-C-A-D also had large negative net charges of -1.64 and -1.45, respectively. In strong contrast, all the carboxy groups of the non-preferred octasaccharides, ΔC-A-D-C and ΔC-C-C-C, had positive net charges. Thus, a large negative net charge was revealed on the carboxy groups in the electronegative zones of the preferred octasaccharides, but not on any carboxy groups of the non-preferred octasaccharides. These results strongly suggest the critical roles of the carboxy group of the C^2 unit of ΔD-C^1-C^2-C^3 and that of the D unit of ΔC-C-A-D for the recognition by the mAb in addition to the sulfate groups on both ends of the octasaccharides.

DISCUSSION

CS chains are heterogeneous in detailed composition, particularly regarding the sulfate content and sulfation pattern as recently revealed by sequencing of a number of oligosaccharides isolated from shark cartilage CS-C (55). It is therefore interesting to define the specific CS structure required for the recognition by this mAb. In this study we have purified and characterized four CS octasaccharide sequences. Among the four sequences, ΔC-C-C-C and ΔC-A-D-C (29) as well as their saturated counterparts (C-C-C-C and C-A-D-C) (55) have been isolated previously from shark cartilage CS-D and CS-C, respectively, after digestion with chondroitinase ABC or testicular hyaluronidase. Although neither ΔD-C-C-C nor ΔC-C-A-D have been reported, their saturated counterparts (D-C-C-C and C-C-A-D) have recently been isolated (55). Among them, two separate octasaccharide sequences (ΔD-C-C-C and ΔC-C-A-D) were specifically recognized by the mAb WF6, and identified as the minimal CS motifs for interaction with WF6. Interestingly anti-CS mAbs such as MO-225, CS-56, LY-111, 2H6 and 473HD or anti-dermatan sulfate mAb 2A12, which were produced by murine

hybridomas also have recently been demonstrated to interact with multiple hexa-, octa- or decasaccharide sequences derived from shark cartilage CS-C, shark cartilage CS-D, squid cartilage CS-E or acidian dermatan sulfate (11, 12, 55, 56). It has recently been demonstrated that a single chain phage display antibody GD3G7 also interacts with multiple decasaccharide sequences isolated from squid cartilage CS-E (63). Although the octasaccharides and the saturated counterparts (D-C-C-C and C-C-A-D), which were recognized by WF6, were isolated in this and previous studies (55) from shark cartilage CS chains, the epitopes are present in humans as elevated levels of the epitopes have been detected by WF6 in sera from patients with osteoarthritis, rheumatoid arthritis (19) and ovarian cancers (20).

In view of the findings that the above-described antibodies, including WF6, interact with multiple oligosaccharides containing similar yet distinct sequences, we used molecular modeling to investigate possible common features shared by the preferred octasaccharides and absent from the non-preferred octasaccharides. The comparison of the structures and sequences of both the two preferred and two non-preferred CS octasaccharides by computer modeling revealed little similarity in the 3D structures or the conformations, but there was considerable similarity in the shapes of the ESP distribution. This appeared to explain their similarity in the binding to the mAb WF6, detected using the oligosaccharide microarray, where ΔD-C-C-C and ΔC-C-A-D showed binding to WF6, but ΔC-C-C-C and ΔC-A-D-C did not (Figs. 6 and 7).

Since hexasaccharides were less inhibitory against the binding of WF6 to CS-PGs (Fig. 1B), there is a clear need for the octasaccharide size for optimal binding. The terminal uronic acid residue in each one of the two preferred octasaccharides is unsaturated and an unnatural structure, which is not present in the immunogen or native CS chains. However, the unsaturated uronic acid residue in each octasaccharide is clearly recognized partially by WF6, as evidenced by the recognition of the 2-*O*-sulfate group on this residue (Figs. 8A and 8B). In addition the reducing terminal GalNAc residue in ΔD-C-C-C and that in ΔC-C-A-D were chemically conjugated with an artificial aminolipid ADHP and thus converted to an unnatural structure. However, the 6-*O*-sulfate group on the GalNAc residue of the C^3 unit of ΔD-C^1-C^2-C^3 and the 6-*O*-sulfate group on the GalNAc residue of the D unit of ΔC-C-A-D were also recognized by WF6 (Figs. 8A and 8B). Thus, it appears that the sulfate groups on the uronic acid and GalNAc derivatives with unnatural saccharide structures are involved in the recognition by the mAb, and the octasaccharide backbones act as platforms to present the critical sulfate groups.

The ESP distributions of ΔD-C-C-C and ΔC-C-A-D, which were recognized by WF6, were very similar (Fig. 8), suggesting that the feature of the recognition by WF6 depends on the electronegative zone shape of the octasaccharides. The RMSD from the average distance between the backbones were not much different in the preferred and non-preferred octasaccharides (Fig. 7), suggesting that the orientation of the sulfate groups and the carboxy groups of the uronic acid residues rather than the sequences of the oligosaccharides influenced the ESP distribution and defines the zone shape. Although the preferred octasaccharides (ΔD-C-C-C and ΔC-C-A-D) have a D unit and a C-C tetrasaccharide in the reverse order, they have similar distribution of the zone shape. The theoretical calculations, based on the shape of the ESP maps of ΔD-C-C-C and ΔC-C-A-D, suggest that the WF6 binding site has a small hydrophilic pocket located on both sides and a large hydrophilic pocket located in the center (Fig. 8). Therefore, it seems that ΔC-C-C-C lacking all these pockets was not recognized. However, ΔC-A-D-C has some similarity to the two preferred octasaccharides, and therefore may be partially recognized by WF6, but the binding force may be weak.

Recent studies (11, 13) on the specificity of anti-CS mAbs MO-225 and CS-56 using several structurally defined octasaccharide sequences have revealed the recognition of not only a common conformation but also the electrostatic feature shared by multiple different octasaccharide sequences by each mAb (11). The conformation analyses on these sequences (13) were performed using ^{1}H-NMR spectroscopy and energy minimization of molecular simulation in the classical mechanics level. The inter-residual distances observed in the NOESY spectrum were in good agreement with the distances calculated in the model for ΔC-A-D-C, suggesting that it is easier for the low energy conformers to be taken *in vitro*. In addition, the charge and electrostatic potential analyses demonstrated that the negative charges are clustered in restricted areas, especially D unit, and the preferred conformers take the advantage to display negative charges in the center of the sequences when flexibility was taken into account. In the present study, we performed the full geometry optimizations for the initial geometries of the four isolated octasaccharides by molecular dynamics calculations including the solvent effect, and then calculated the ESP distribution based on the NAO-PC model. The semi-empirical molecular orbital calculation, which is much more accurate than the charge and electrostatic potential analyses previously used, revealed new electrostatic features that the preferred octasaccharides have a similar electronegative zone shape, which is caused by the orientation and the negative charges of the oxygen atoms of the sulfate groups and the carboxy groups. Based on these results, we could predict three candidates for the WF6 binding sites in the center and at both ends of each preferred octasaccharide

sequence, to substantiate and extend the previous findings for the anti-CS mAbs MO-225 and CS-56 (13) that the exo-cyclic negatively charged tails play an important role caused by the negative charges of the oxygen atoms of the carboxy groups and the sulfate groups with classical ESP. Furthermore, the computational simulations in the present study clearly demonstrated that the octasaccharides having the large negative net charges (less than -1.30) of both the sulfate groups and the carboxy groups could be recognized by the mAb. In the case of ΔD-C^1-C^2-C^3, the 2-*O*-sulfate on the ΔD unit, the 6-*O*-sulfate on the C^3 unit and the carboxy group on the C^2 unit are particularly important, whereas in the case of ΔC^1-C^2-A-D, the 6-*O*-sulfate of the ΔC^1 unit, the 2-*O*- and 6-*O*-sulfate groups and the carboxy group on the D unit are critical. Thus, the present study has suggested for the first time the importance of assessing the magnitude and sign of the atomic point charges on ESP to reveal the critical functional groups in the molecular recognition of sulfated oligosaccharides by monoclonal antibodies.

As demonstrated in this study, the quantum chemical approach brings a more complete analysis of the various conformations and electrostatic properties of CS oligosaccharides compared with classical mechanics methods. This approach will enable future studies to address the complex problems presented by the dynamic behavior of sugar structures using QM/MM combined *ab initio* calculation and molecular dynamics simulation and will give a deeper understanding of the relationships amongst conformations, electrostatic properties and motion of GAG oligosaccharides, which determine their *in vivo* functions.

Acknowledgements
We thank Accelrys K. K. for the use of Accelrys Material Studio software, and Shuji Mizumoto (Hokkaido University) for sugar analysis of fraction C6Ep1.

REFERENCES

1. Letourneau, P. C., Condic, M. L., and Snow, D. M. (1992) *Curr. Opin. Genet. Dev.* **2,** 625-634
2. Reichardt, L. F., and Tomaselli, K. J. (1991) *Annu. Rev. Neurosci.* **14,** 531-570
3. Hardingham, T. E., and Fosang, A. J. (1992) *FASEB J.* **6,** 861-870
4. Sugahara, K., Mikami, T., Uyama, U., Mizuguchi, S., Nomura, K., and Kitagawa, H. (2003) *Curr. Opin. Struct. Biol.* **13**, 612-620
5. Brown, M. P., West, L. A., Merritt, K. A., and Plaas, A. H. (1998) *Am. J. Vet. Res.* **59,** 786-791
6. Clement, A. M., Nadanaka, S., Masayama, K., Mandl, C., Sugahara, K., and Faissner, A. (1998) *J. Biol. Chem.* **273,** 28444-28453
7. Clement, A. M., Sugahara, K., and Faissner, A. (1999) *Neurosci. Lett.* **269,** 125-128
8. Kawashima, H., Atarashi, K., Hirose, M., Hirose, J., Yamada, S., Sugahara, K., and Miyasaka, M. (2002) *J. Biol. Chem.* **277,** 12921-12930
9. Kitagawa, H., Ujikawa, M., Tsutsumi, K., Tamura, J., Neumann, K. W., Ogawa, T., and Sugahara, K. (1997) *Glycobiology* **7,** 905-911
10. Caterson, B., Griffin, J., Mahmoodian, F., and Sorrell, J. M. (1990) *Biochem. Soc. Trans.* **18,** 820-823
11. Ito, Y., Hikino, M., Yajima, Y., Mikami, T., Sirko, S., von, H. A., Faissner, A., Fukui, S., and Sugahara, K. (2005) *Glycobiology* **15,** 593-603
12. Bao, X., Pavão, M.S.G., dos Santos, J. C., and Sugahara, K. (2005) *J. Biol. Chem.* **280,** 23184-23193
13. Blanchard, V., Chevalier, F., Imberty, A., Leeflang, B. R., Basappa, Sugahara, K., and Kamerling, J. P. (2007) *Biochemistry* **46,** 1167-1175
14. Sorrell, J. M., Mahmoodian, F., Schafer, I. A., Davis, B., and Caterson, B. (1990) *J. Histochem. Cytochem.* **38,** 393-402
15. Mark, M. P., Baker, J. R., Morrison, K., and Ruch, J. V. (1990) *Differentiation* **43,** 37-50
16. Fernaud-Espinosa, I., Nieto-Sampedro, M., and Bovolenta, P. (1996) *J. Neurobiol.* **30,** 410-424
17. Caterson, B., Mahmoodian, F., Sorrell, J. M., Hardingham, T. E., Bayliss, M. T., Carney, S. L., Ratcliffe, A., and Muir, H. (1990) *J. Cell Sci.* **97 (Pt 3),** 411-417
18. Johnson, K. A., Hay, C. W., Chu, Q., Roe, S. C., and Caterson, B. (2002) *Am. J. Vet. Res.* **63,** 775-781
19. Pothacharoen, P., Teekachunhatean, S., Louthrenoo, W., Yingsung, W., Ong-Chai, S., Hardingham, T., and Kongtawelert, P. (2006) *Osteoarthritis Cartilage* **14**, 299-301
20. Pothacharoen, P., Ong-Chai, S.,Supaphun, J., Kumja, P., Wanaphirak, C., Sugahara, K., Hardingham, T., and Kongtawelert, P. (2006) *J. Biochem.* **140,** 517-524
21. Hazell, P. K., Dent, C., Fairclough, J. A., Bayliss, M. T., and Hardingham, T. E. (1995) *Arthritis Rheum.* **38,** 953-959
22. Lohmander, L. S. (1991) *Acta Orthop. Scand.* **62,** 623-632
23. Lewis, S., Crossman, M., Flannelly, J., Belcher, C., Doherty, M., Bayliss, M. T., and Mason, R. M. (1999) *Ann. Rheum. Dis.* **58,** 441-445

24. Lohmander, L. S., and Felson, D. T. (1997) *J. Rheumatol.* **24,** 782-785
25. Kongtawelert, P., Hardingham, T., Ong-chai, S., Sugahara, K., Pothacharoen, P., and Tiengburanathum, N. (5 A.D.) Antibody specific for a chondroitin sulfate epitope, WO 2005/118645 A1 ed.
26. Sorrell, J. M., Carrino, D. A., and Caplan, A. I. (1993) *Matrix* **13,** 351-361
27. Hardingham, T. E., Fosang, A. J., Hey, N. J., Hazell, P. K., Kee, W. J., and Ewins, R. J. (1994) *Carbohydr. Res.* **255,** 241-254
28. Li, H., and Schwartz, N. B. (1995) *J. Mol. Evol.* **41,** 878-885
29. Nadanaka, S., Clement, A., Masayama, K., Faissner, A., and Sugahara, K. (1998) *J. Biol. Chem.* **273,** 3296-3307
30. Avnur, Z., and Geiger, B. (1984) *Cell* **38,** 811-822
31. Mark, M. P., Butler, W. T., and Ruch, J. V. (1989) *Dev. Biol.* **133,** 475-488
32. Caterson, B., Hughes, C. E., Roughley, P., and Mort, J. S. (1995) *Acta Orthop. Scand. Suppl.* **266,** 121-124
33. Heinegard, D. (1977) *J. Biol. Chem.* **252,** 1980-1989
34. Bitter, M., and Muir, H. (1962) *Anal. Biochem.* **4**, 330-334
35. Juhasz, P., and Biemann, K. (1995) *Carbohydr. Res.* **270**, 131-147
36. Bigge, J. C., Patel, T. P., Bruce, J. A., Goulding, P. N., Charles, S. M., and Parekh, R. B. (1995) *Anal. Biochem.* **230,** 229-238
37. Kinoshita, A., and Sugahara, K. (1999) *Anal. Biochem.* **269,** 367-378
38. Yamaguchi, K., Tamaki, H., and Fukui, S. (2006) *Glycoconj. J.* **23,** 513-523
39. Stoll, M. S., Feizi, T., Loveless, R. W., Chai, W., Lawson, A. M., and Yuen, C. T. (2000) *Eur. J. Biochem.* **267,** 1795-1804
40. Yamagata, T., Saito, H., Habuchi, O., and Suzuki, S. (1968) *J. Biol. Chem.* **243,** 1523-1535
41. Rappe, A. K., Casewit, C. J., Colwell, K. S., Goddard, W. A., and Skiff, W. M. (1992) *J. Am. Chem. Soc.* **114**, 10024-10035
42. Rappe, A. K., Colwell, K. S., and Casewit, C. J. (1993) *Inorg. Chem.* **32**, 3438-3450
43. Klamt, A., and Schuurmann, G. (1993) *J. Chem. Soc. Perkin Trans.* **2**, 799-805
44. Tomasi, J., and Persico, M. (1994) *Chem. Rev.* **94**, 2027-2094
45. Thiel, W, and Voityuk, A. A. (1996) *J. Phys. Chem.* **100**, 616-626; Thiel, W., and Voityuk, A. A. (1994) *THEOCHEM* **119**, 141-154; Thiel, W., and Voityuk, A. A. (1992) *Theoretica Chimica Acta* **81**, 391-404 (with an erratum in (1996) *Theoretica Chimica Acta* **93**, 315)
46. Voityuk, A. A., and Roesch, N. (2000) *J. Phys. Chem.* A **104**, 4089-4094
47. Clark, T., Breindl, A., and Rauhut, G. (1995) *J. Mol. Model.* **1**, 22-35
48. Rauhut, G., Clark, T., and Steinke, T. (1993) *J. Am. Chem. Soc.* **115**, 9174-9181
49. Rauhut,G., and Clark, T. (1993) *J. Comput. Chem.* **14**, 503-509
50. Dewar, M. J. S., Zoebisch, E. G., Healy, E. F., and Stewart, J. J. P. (1985) *J. Am. Chem. Soc.* **107**, 3902-3909
51. Baker, J. (1986) *J. Comput. Chem.* **7**, 385-395
52. Rauhut, G., and Clark, T. (1993) *J. Am. Chem. Soc.* **115**, 9127-9135
53. Nandini, C. D., and Sugahara, K. (2006) In *Advances in Pharmacology* (Volpi, N., ed.) vol 53, pp. 253-279, Elsevier, UK
54. Bao, X., Muramatsu, T., and Sugahara, K. (2005) *J. Biol. Chem.* **280,** 35318-35328
55. Deepa, S. S., Yamada, S., Fukui, S., and Sugahara, K. (2007) *Glycobiology* **17**, 631-645
56. Deepa, S. S., Kalayanamitra, K., Ito, Y., Kongtaweelert, P., Fukui, S., Yamada, S., Mikami, T., and Sugahara, K. (2007) *Biochemistry* **46,** 2453-2465
57. Sugahara, K., Tanaka, Y., and Yamada, S. (1996) *Glycoconj. J.* **13,** 609-619
58. Sugahara, K., Shigeno, K., Masuda, M., Fujii, N., Kurosaka, A., and Takeda, K. (1994) *Carbohydr. Res.* **255,** 145-163
59. Sugahara, K., Nadanaka, S., Takeda, K., and Kojima, T. (1996) *Eur. J. Biochem.* **239,** 871-880
60. Nadanaka, S., and Sugahara, K. (1997) *Glycobiology* **7,** 253-263
61. Mulliken, R. S. (1955) *J. Chem. Phys.* **23**, 1833-1840
62. Polizer, P., and Murray, J. S. (1991) In *Reviews in Computational Chemistry* (Lipkowitz, K. B. and Boyd, D. B., ed.) vol. 2, pp. 273-312, VCH Publishers, New York
63. Purushothaman, A., Fukuda, J., Mizumoto, S., ten Dam, G. B., van Kuppevelt, T. H., Kitagawa, H., Mikami, T., and Sugahara, K. (2007) *J. Biol. Chem.*, **282,** 19442-19452

FOOTNOTES

*The work in Japan was supported in part by the Scientific Research Promotion Fund from the Japan Private School Promotion Foundation, the Core Research for Evolutional Science and Technology (CREST) of the Japan Science and Technology (JST) Agency (to K. S.), the New Energy and Industrial Technology Development Organization (NEDO) to (K. S.) and The Human Frontier Science Program (to K. S.). The work in Thailand was supported by Basic Research Grant to PK, BRG4680004 from The Thailand Research Fund, The Royal Golden Jubilee Ph.D. Program PHD/0121/2544 (to PP) and PHD/0225/2545 (to KK), and the National Research Council of Thailand. TH acknowledges the support of The Wellcome Trust.

[1]These authors contributed equally to this work.

[2]To whom correspondence may be addressed: Thailand Excellence Center for Tissue Engineering, Department of Biochemistry, Faculty of Medicine, Chiang Mai University, Chiang Mai, 50200, Thailand. Tel: 66-(53)-894188, Fax: 66-(53)-894188, E-mail: pkongtaw@mail.med.cmu.ac.th.

[3]To whom correspondence may be addressed: Laboratory of Proteoglycan Signaling and Therapeutics, Frontier Research Center for Post-Genomic Science and Technology, Hokkaido University Graduate School of Life Science, Nishi 11-choume, Kita 21-jo, Kita-ku, Sapporo, Hokkaido 001-0021, Japan, Tel: +81-(0)11-706-9054; Fax: +81-(0)11-706-9056, E-mail: k-sugar@sci.hokudai.ac.jp.

[4]The abbreviations used in this paper are: CS, chondroitin sulfate; DS, dermatan sulfate; GAG, glycosaminoglycan; PG, proteoglycan; GlcUA, D-glucuronic acid; GalNAc, *N*-acetyl-D-galactosamine; HexUA, hexuronic acid; IdoUA, L-iduronic acid; 2S, 2-*O*-sulfate; 4S, 4-*O*-sulfate; 6S, 6-*O*-sulfate; ELISA, enzyme–linked immunosorbent assay; BSA, bovine serum albumin; HPLC, high performance liquid chromatography; HRP, horseradish peroxidase; DAB, 3, 3'-diaminobenzidine.

FIGURE LEGENDS

Fig. 1. Fractionation of a partial chondroitinase digest of a commercial CS-C preparation from shark cartilage by size exclusion chromatography and the reactivity of the fractions with the mAb WF6. *A*, The partial chondroitinase ABC digest of a commercial CS-C preparation was chromatographed on a column (1.6 x 90 cm) of Bio-Gel P-6 using 0.2 M ammonium acetate as eluent. Fractions (2.0 ml) were monitored by absorbance at 232 nm. Fractions C1 to C9 were pooled as indicated and dialyzed against water. *B*, Each peak obtained in panel A was assayed for its inhibitory activity by competitive ELISA against the binding of mAb WF6 to the shark aggrecan aggregate (A_1 fraction) using the sample corresponding to 200 μg (filled bar), 100 μg (grey bar) or 50 μg (open bar) of uronic acid. All values represent the mean ± S.D. from three independent experiments in duplicate. The percent inhibition was calculated as follows: % Inhibition = 100 – [([OD_{test} – OD_{blank}]/ [$OD_{control}$-OD_{blank}]) x 100].

Fig. 2. Subfractionation of the oligosaccharide fraction C6 by strong anion-exchange (SAX) FPLC. *A*, The oligosaccharide fraction C6 obtained by gel filtration (Fig. 1A) was subfractionated by strong anion-exchange (SAX) FPLC on a monoQ cartridge column using a linear gradient of $LiClO_4$. Subfractions were collected at the peaks indicated by A-E. *B*, The reactivity of the oligosaccharide subfractions obtained in panel A with the mAb WF6 was evaluated by competitive ELISA against the binding of the mAb WF6 to the immobilized CS-PG aggrecan preparation (A_1 fraction) from shark cartilage. The assays were carried out using the samples equivalent to 200 μg (filled bar) or 100 μg of uronic acid (open bar). All values represent the mean ± S.D. from three independent experiments in duplicate. The percent inhibition was calculated as in Fig. 1. *C*, Demonstration of the direct binding of the mAb WF6 to the oligosaccharides in the SAX subfractions by oligosaccharide microarray. The ADHP-derivatized SAX subfractions (6A-6E) were derivatized with a fluorescent lipid ADHP as described in "Experrimenral Procedures", spotted on a nitrocellulose membrane (1.0 pmol/spot) and probed with mAb WF6. The immobilization of the oligosaccharides was detected by fluorescence under UV light, and the binding of WF6 was detected by HRP-conjugated mouse anti-IgM and DAB.

Fig. 3. Purification of the octasaccharide subfractions C6C, C6D and C6E by anion-exchange HPLC. The SAX subfractions of CS-C octasaccharides (C6C, C6D and C6E), which were obtained by monoQ FPLC (Fig. 2A), were further subfractionated individually by anion-exchange HPLC on an amine-bound silica column using elution by a linear gradient of Na_2HPO_4. The peaks C6Cp1, C6Dp1, and C6Ep1-C6Ep3 were collected as indicated.

Fig. 4. **Chondroitinase ABC digestion of fraction C6Ep2**. The 2AB-derivative of fraction C6Ep2 was analyzed before (panel A) and after digestion (panel B) with chondroitinase ABC by anion-exchange HPLC on an amine-bound silica column using a linear gradient of NaH_2PO_4 from 16 mM to 1.0 M over 90 min. The chondroitinase ABC digest was labeled with 2AB again, and analyzed (C) to identify the disaccharide units from the non-reducing terminal and the internal position. The elution positions of authentic unsaturated 2AB-labeled disaccharides are indicated in the *top panel* by *arrows*. a, ΔO; b, ΔC; c, ΔA; d, ΔD; e, ΔE; f, ΔT; g, authentic tetrasaccharide ΔA-D (57). The open arrow indicates the major octasaccharide in fraction C6Ep2.

Fig. 5. Oligosaccharide microarray analysis of binding of WF6 to the isolated octasaccharide fractions. Fractions C6E1-C6Ep3 purified by anion-exchange HPLC (Fig. 3) were derivatized with fluorescent aminolipid ADHP together with authentic C-C-A-D (55), spotted on a nitrocellulose membrane (5.0 picomoles/spot) for fluorescence detection, and then probed with mAb WF6, followed by detection with mouse anti-IgM conjugated with HRP and DAB.

Fig. 6. Optimized structures of the isolated CS octasaccharides by computational analysis. Optimized structures were drawn by stick-model and solvent surface (see "Experimental Procedures"). *A*, ΔD-C-C-C (preferred); *B*, ΔC-C-A-D (preferred); *C*, ΔC-A-D-C (non-preferred); *D*, ΔC-C-C-C (non-preferred).

Fig. 7. Superimposed structures of the preferred and non-preferred CS octasaccharides. *A*, ΔD-C-C-C (red) and ΔC-C-A-D (yellow); *B*, ΔD-C-C-C (red) and ΔC-A-D-C (yellow); *C*, ΔD-C-C-C (red) and ΔC-C-C-C (yellow); *D*, ΔC-C-A-D (red) and ΔC-A-D-C (yellow); *E*, ΔC-C-A-D and ΔC-C-C-C. Structures were generated and optimized as described in "Experimental Procedures".

Fig. 8. Calculated ESP distribution of the isolated CS octasaccharides. ESP distribution was calculated for each isolated octasaccharide, and the electronegative zone (yellow) and electropositive zone (blue) are shown. *A*, ΔD-C-C-C (preferred); *B*, ΔC-C-A-D (preferred); *C*, ΔC-A-D-C (non-preferred); *D*, ΔC-C-C-C (non-preferred).

The predicted binding sites of the two octasaccharide sequences, ΔD-C-C-C and ΔC-C-A-D, which are recognized by WF6, are indicated by red circles in *A* and *B*. The iso-values are 0.6 eV for the iso-surface of the electropositive zone and -0.6 eV for that of the electronegative zone.

Scheme 1. Strategy for exo-sequencing of CS-C octasaccharides.

Table I

The yield, purity and disaccharide composition of the subfractions of C6 obtained by SAX FPLC

SAX Subfraction	Yield [a] (mg)	Purity (%)[b]	Disaccharides formed (mole %) Unsaturated
C6A	1.0	65.6	△O (12), △C (76), △A (10)
C6B	1.9	49.8	△O (1), △C (82), △A (17)
C6C	2.9	80.7	△C (88), △A (12)
C6D	1.0	53.5	△C (80), △A (19.3), △D (1.4)
C6E	2.0	82.2	△O (2.6), △C (55), △A (26), △D (17)

[a]One gram of CS-C was partially digested with chondroitinase ABC and 13 mg of fraction C was obtained by gel filtration (Fig. 1A). Eleven mg of fraction C was subfractionated by SAX FPLC (Fig. 2A) and the yields of the subfractions are shown.

[b]The percent purity was calculated based on the peak area of the major peak area on the HPLC chromatogram.

[c]The abbreviations used: ΔO unit, ΔHexUAα1-3GalNAc; ΔA unit, ΔHexUAα1-3GalNAc(4S); ΔC unit, ΔHexUAα1-3GalNAc(6S); ΔD unit, ΔHexUA(2S)α1-3GalNAc(4S).

Table II

MALDI-TOF MS analysis of the subfractions of C6 obtained by SAX HPLC

Fractions	Oligosaccharides (*m/z*)[b]			Deduced sugar and sulfate Composition
	Mass Observed For the Complex	Observed mass[c]	Theoretical Mass[d]	
C6A[a]	No signal			
C6B	No signal			
C6C	5062.73	1,844.73	1,836	$\Delta HexUA_4HexNAc_4(SO_3H)_4$
C6D	5062.45	1844.45	1,836	$\Delta HexUA_4HexNAc_4(SO_3H)_4$
	5155.91	1937.91	1,938	$\Delta HexUA_4HexNAc_4(SO_3H)_4\ SO_3Na$
C6E	5142.57	1924.57	1,916	$\Delta HexUA_4HexNAc_4(SO_3H)_5$
	5234.88	2016.88	2,018	$\Delta HexUA_4HexNAc_4(SO_3H)_5\ SO_3Na$

[a] Each oligosaccharide fraction (10 pmol) was mixed with an equimolar amount of a basic peptide $(Arg\text{-}Gly)_{15}$ followed by mixing with a matrix gentisic acid, and the spectrum was recorded in a positive ion mode.

[b] The m/z value of the protonated 1:1 complex of each oligosaccharide and the basic peptide $(Arg\text{-}Gly)_{15}$.

[c] The observed mass of each oligosaccharide obtained by subtracting the value of the protonated peptide (3,218) from the protonated 1:1 complex.

[d] The theoretical mass calculated for each deduced structure.

Table III

The yield, purity and disaccharide composition of the subfractions of C6C, C6D and C6E obtained by SAX HPLC

Subfraction	Yield[a] (nmol)	Purity[b] (%)	Disaccharides formed[c] (mole %)	Possible sequence[d]
C6Cp1[a]	43.8	95	ΔC (100)	ΔC-C-C-C
C6Dp1	7.0	100	ΔC (100)	ΔC-C-C-C
C6Ep1	9.4	100	ΔC (76), ΔD (24)	ΔD-C-C-C
C6Ep2	10.0	68	ΔC (71), ΔD (16), ΔA (13)	ΔC-C-A-D
C6Ep3	11.8	100	ΔC (55), ΔD (17), ΔA (26)	ΔC-A-D-C

[a]Fractions C6C (100 nmol), C6D (25 nmol) and C6E (35 nmol) were individually subjected to anion-exchange HPLC (Fig. 3) and the amounts of the purified fractions quantified by absorbance at 232 nm are shown.

[b]Each fraction was labeled with 2AB, purified by paper chromatography (12) and examined for its purity by anion-exchange HPLC on an amine-bound silica column. The percent purity was calculated based on the peak area on the chromatogram.

[c]Disaccharide analysis was performed after digestion with chondroitinase ABC and subsequent labeling with 2AB followed by anion-exchange HPLC (For details, see "Experimental Procedures").

[d]For the sequencing of the major octasaccharide in each fraction, see the text.

Table IV

Reducing terminal di-and tetrasaccharide released from 2AB-derivatized octasaccharides by digestion with chondroitinase AC-II or ABC[a]

Fractions	Chondroitinase AC-II	Chondroitinase ABC
	2AB-labeled unsaturated saccharides detected (mole%)	
C6Cp1	ΔC (82), ΔA (11), ΔD (7)	ΔC-C (100)
C6Ep1	ΔC (100)	ΔC-C (89), ΔD-C (11) [ΔC-C-C (15), ΔD-C-C-C (85)][b]
C6Ep2	ΔA-D (100)	ΔA-D (100)
C6Ep3	ΔC (100)	ΔC-C (12), ΔD-C (88)

[a]Each fraction was labeled with 2AB, purified by paper chromatography to remove excess 2AB-derivatizing reagents and was digested separately with chondroitinase AC-II or ABC. Each digest was analyzed by anion-exchange HPLC on an amine-bound silica column to determine the reducing terminal sequences of the major and minor components in each fraction.

[b]2AB-labeled C6Ep1 was partially digested with a highly purified chondroitinase ABC preparation (see Experimental Procedures"), and analyzed as described above.

Table V

Di- and tetrasaccharides released from 2AB-derivatized octasaccharides by chondroitinase AC-II and ABC

Each octasaccharide fraction was labeled with 2AB at the reducing terminal and was digested separately with chondroitinase AC-II or ABC. After the digest was further labeled with 2AB, the 2AB-labeled oligosaccharides were purified to remove excess 2AB-derivatizing reagents, and then analyzed by anion-exchange HPLC on an amine-bound silica column.

Fractions	Chondroitinase AC-II	Chondroitinase ABC
	2AB-labeled unsaturated saccharides detected (mole%)	
C6Cp1	Δ**C (86)**[a], ΔA (9), ΔD (3), ΔE (2)	ΔC (42), Δ**C-C (58)**
C6Ep1	Δ**C (71)**, ΔD (29)	ΔC (15), ΔD (38), Δ**C-C (39)**, ΔD-C (5), ΔD-A (3) [ΔD (6), ΔC-C-C (14), Δ**D-C-C-C (80)**][b]
C6Ep2	Δ**C (66)**, ΔA (2), ΔA-D (32)	Δ**C (65)**, ΔA (4), ΔA-D (31)
C6Ep3	Δ**C (65)**, ΔA (18), ΔD (17)	Δ**C (35)**, ΔA (27), ΔC-C (3), Δ**D-C (35)**

[a]Di- or tetrasaccharide units in bold letters indicate the major component released by each digestion.

[b]2AB-labeled C6Ep1 was partially digested by a highly purified chondroitinase ABC preparation (see "Experimental Procedures"), and analyzed as described above for identification of the ΔC-C-C product (see the text).

Table VI

(A) Optimized dihedral angles of the disaccharides in the local energy minima

GlcUA-GalNAc(6S)			GlcUA-GalNAc(4S)			GlcUA(2S)-GalNAc(6S)			GalNAc(6S)-GlcUA			GalNAc(4S)-GlcUA(2S)		
φ	ψ	FE/kcal/mol	φ	ψ	FE/kcal/mol	φ	ψ	FE/kcal/mol	φ	ψ	FE/kcal/mol	φ	ψ	FE/kcal/mol
70	99	-846.3	93	147	-838.7	69	109	-1099.4	63	89	-836.7	58	79	-1093.3
281	78	-846.6	276	127	-838.3	295	114	-1102.1	301	92	-845.6	303	94	-1097.8
72	310	-839.3	86	302	-326.9	68	314	-1095.1	50	238	-846.5	53	236	-1096.2
279	262	-845.4	274	289	-837.6	260	282	-1099.2	301	241	-846.2	254	214	-1094.3

Twenty-four initial conformations were chosen for each CS disaccharide in the range of (40°-330°, 60°-330°) and then full geometry optimizations were performed using the semi-empirical molecular orbital calculations taking the solvent effects into account. The results obtained for all the twenty-four conformations of each CS disaccharide are summarized in Supplemental Table S1. The (ϕ, ψ) values and the formation energies in the local energy minima around (80°, 100°), (300°, 100°), (80°, 300°), and (300°, 300°) (ref. 13), have been used for Table VIA. FE stands for the formation energy.

(B) Optimized dihedral angels (ϕ, ψ) of the disaccharide constituents in the four octasaccharide sequences

	8-7		7-6		6-5		5-4		4-3		3-2		2-1*	
	φ	ψ	φ	ψ	φ	ψ	φ	ψ	φ	ψ	φ	ψ	φ	ψ
ΔCADC	270	78	283	244	292	107	296	246	292	130	282	249	272	129
ΔCCAD	291	120	298	243	284	98	282	247	281	126	299	236	279	94
ΔCCCC	272	140	260	56	263	59	304	240	276	77	272	208	257	60
ΔDCCC	279	85	288	90	274	139	311	267	292	86	265	207	312	155

The individual octasaccharides were modeled based on the information about the dihedral angels of the constituent disaccharides according to the previous study (13) using Accelrys Materials Studio's module, and about one hundred conformations in the local energy minima were obtained for each octasaccharide to search for the global minimum using the anneal dynamics optimization with the Forcite module. A full geometry optimization was then performed for the global minimum conformation as the initial geometry, using the semi-empirical molecular orbital method to obtain the final conformation of each octasaccharide.

*Eight sugar residues of each octasaccharide sequence have been numbered 1 to 8 from the reducing end as in ref. 13.

Table VII

Atomic point charges on ESP of the sulfate groups of the four isolated CS octasaccharides

Sequence	S (2S)	O1 (2S)	O2 (2S)	O3 (2S)	Sum (2S)	S (4S)	O1 (4S)	O2 (4S)	O3 (4S)	Sum (4S)	S (6S)	O1 (6S)	O2 (6S)	O3 (6S)	Sum (6S)
Δ**D**CCC	**+8.27**	**-3.00**	**-3.34**	**-3.35**	**-1.42**	**-**	**-**	**-**	**-**	**-**	**+4.45**	**-1.21**	**-1.38**	**-2.37**	**-0.51**
ΔD**C**CC	**-**	**-**	**-**	**-**	**-**	**-**	**-**	**-**	**-**	**-**	**+7.11**	**-1.24**	**-2.53**	**-2.61**	**+0.73**
ΔDC**C**C	**-**	**-**	**-**	**-**	**-**	**-**	**-**	**-**	**-**	**-**	**+6.69**	**-2.14**	**-2.57**	**-2.84**	**-0.86**
ΔDCC**C**	**-**	**-**	**-**	**-**	**-**	**-**	**-**	**-**	**-**	**-**	**+8.44**	**-2.67**	**-3.36**	**-3.71**	**-1.30**
Δ**C**CAD	**-**	**-**	**-**	**-**	**-**	**-**	**-**	**-**	**-**	**-**	**+6.20**	**-2.47**	**-2.71**	**-2.86**	**-1.84**
ΔC**C**AD	**-**	**-**	**-**	**-**	**-**	**-**	**-**	**-**	**-**	**-**	**+8.33**	**-2.31**	**-2.96**	**-3.39**	**-0.33**
ΔCC**A**D	**-**	**-**	**-**	**-**	**-**	**+5.02**	**-1.53**	**-2.11**	**-2.53**	**-1.15**	**-**	**-**	**-**	**-**	**-**
ΔCCA**D**	**+5.04**	**-1.86**	**-2.19**	**-2.53**	**-1.54**	**-**	**-**	**-**	**-**	**-**	**+7.71**	**-2.82**	**-2.91**	**-3.34**	**-1.36**
Δ**C**ADC	**-**	**-**	**-**	**-**	**-**	**-**	**-**	**-**	**-**		**+6.36**	**-1.66**	**-2.37**	**-3.20**	**-0.87**
ΔC**A**DC	**-**	**-**	**-**	**-**	**-**	**+2.04**	**-0.57**	**-1.04**	**-1.76**	**-1.33**	**-**	**-**	**-**	**-**	**-**
ΔCA**D**C	**+4.48**	**-1.60**	**-1.92**	**-2.23**	**-1.27**	**-**	**-**	**-**	**-**	**-**	**+6.79**	**-2.01**	**-2.71**	**-3.07**	**-1.00**
ΔCAD**C**	**-**	**-**	**-**	**-**	**-**	**-**	**-**	**-**	**-**	**-**	**+7.71**	**-2.82**	**-2.91**	**-3.34**	**-1.36**
Δ**C**CCC	**-**	**-**	**-**	**-**	**-**	**-**	**-**	**-**	**-**	**-**	**+5.89**	**-1.73**	**-1.80**	**-2.54**	**-0.18**
ΔC**C**CC	**-**	**-**	**-**	**-**	**-**	**-**	**-**	**-**	**-**	**-**	**+5.37**	**-1.45**	**-1.82**	**-2.40**	**-0.30**
ΔCC**C**C	**-**	**-**	**-**	**-**	**-**	**-**	**-**	**-**	**-**	**-**	**+4.51**	**-1.74**	**-1.94**	**-2.00**	**-1.17**
ΔCCC**C**	**-**	**-**	**-**	**-**	**-**	**-**	**-**	**-**	**-**	**-**	**+7.30**	**-2.54**	**-2.65**	**-3.03**	**-0.92**

Table VIII

(A) Mulliken atomic charges of the carboxy groups of the four isolated CS octasaccharides[a]

	The first carboxy group[b]					The second carboxy group					The third carboxy group					The fourth carboxy group				
Sequence	**C**	**=O**	**-O-**	**H**	**Sum**	**C**	**=O**	**-O-**	**H**	**Sum**	**C**	**=O**	**-O-**	**H**	**Sum**	**C**	**=O**	**-O-**	**H**	**Sum**
ΔDCCC	**0.43**	**-0.47**	**-0.39**	**0.34**	**-0.09**	**0.45**	**-0.47**	**-0.39**	**0.34**	**-0.07**	**0.42**	**-0.47**	**-0.38**	**0.35**	**-0.08**	**0.43**	**-0.41**	**-0.40**	**0.34**	**-0.04**
ΔCCAD	**0.43**	**-0.47**	**-0.38**	**0.34**	**-0.08**	**0.43**	**-0.45**	**-0.39**	**0.35**	**-0.06**	**0.42**	**-0.50**	**-0.37**	**0.35**	**-0.10**	**0.43**	**-0.49**	**-0.39**	**0.34**	**-0.11**
ΔCADC	**0.44**	**-0.52**	**-0.37**	**0.35**	**-0.10**	**0.42**	**-0.48**	**-0.39**	**0.34**	**-0.11**	**0.42**	**-0.50**	**-0.38**	**0.35**	**-0.11**	**0.42**	**-0.49**	**-0.37**	**0.35**	**-0.09**
ΔCCCC	**0.44**	**-0.48**	**-0.39**	**0.35**	**-0.08**	**0.40**	**-0.49**	**-0.38**	**0.34**	**-0.13**	**0.43**	**-0.44**	**-0.39**	**0.33**	**-0.07**	**0.40**	**-0.47**	**-0.38**	**0.34**	**-0.11**

[a]Mulliken atomic charges were calculated according to the method reported in ref. (61).
[b]The four carboxy groups are numbered from the non-reducing end to the reducing end.

(B) ESP atomic point charges of the carboxy groups of the four isolated CS octasaccharides[a]

	The first carboxy group[b]					The second carboxy group					The third carboxy group					The fourth carboxy group				
Sequence	**C**	**=O**	**-O-**	**H**	**Sum**	**C**	**=O**	**-O-**	**H**	**Sum**	**C**	**=O**	**-O-**	**H**	**Sum**	**C**	**=O**	**-O-**	**H**	**Sum**
ΔDCCC	**4.84**	**-1.86**	**-1.60**	**-0.13**	**1.25**	**3.22**	**-1.92**	**-1.66**	**0.02**	**-0.33**	**-1.06**	**-0.35**	**0.37**	**-0.60**	**-1.64**	**3.34**	**-1.42**	**-2.13**	**2.27**	**2.06**
ΔCCAD	**4.61**	**-2.27**	**-1.98**	**0.82**	**1.18**	**-0.04**	**-0.69**	**0.41**	**0.32**	**0.00**	**1.08**	**-0.49**	**0.19**	**-0.30**	**0.48**	**0.32**	**-0.71**	**-1.80**	**0.74**	**-1.45**
ΔCADC	**9.60**	**-3.60**	**-0.82**	**-1.31**	**3.88**	**1.04**	**-0.50**	**-0.31**	**0.02**	**0.25**	**2.77**	**-0.83**	**-0.20**	**-0.44**	**1.30**	**2.43**	**-0.56**	**-0.39**	**-0.23**	**1.25**
ΔCCCC	**6.50**	**-2.45**	**-2.85**	**0.81**	**2.01**	**5.10**	**-2.70**	**-1.36**	**0.07**	**1.10**	**2.21**	**-0.96**	**-0.88**	**0.13**	**0.50**	**3.18**	**-1.16**	**-1.88**	**1.54**	**1.69**

[a]ESP atomic point charges were calculated according to the method reported in ref. (62).
[b]The four carboxy groups are numbered from the non-reducing end to the reducing end.

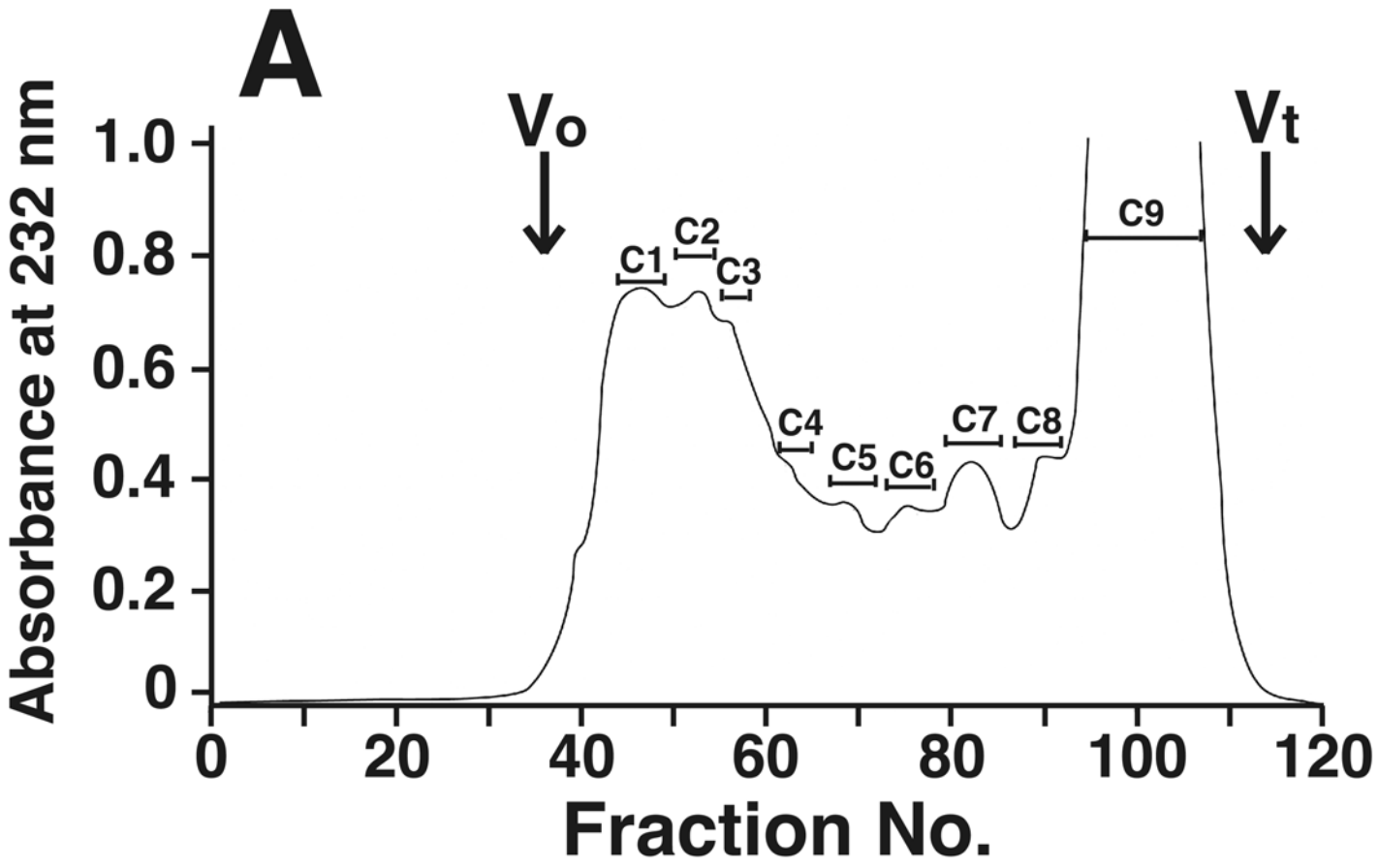
A
Vo
Vt
C1
C2
C3
C4
C5
C6
C7
C8
C9
Absorbance at 232 nm
1.0
0.8
0.6
0.4
0.2
0
0
20
40
60
80
100
120
Fraction No.

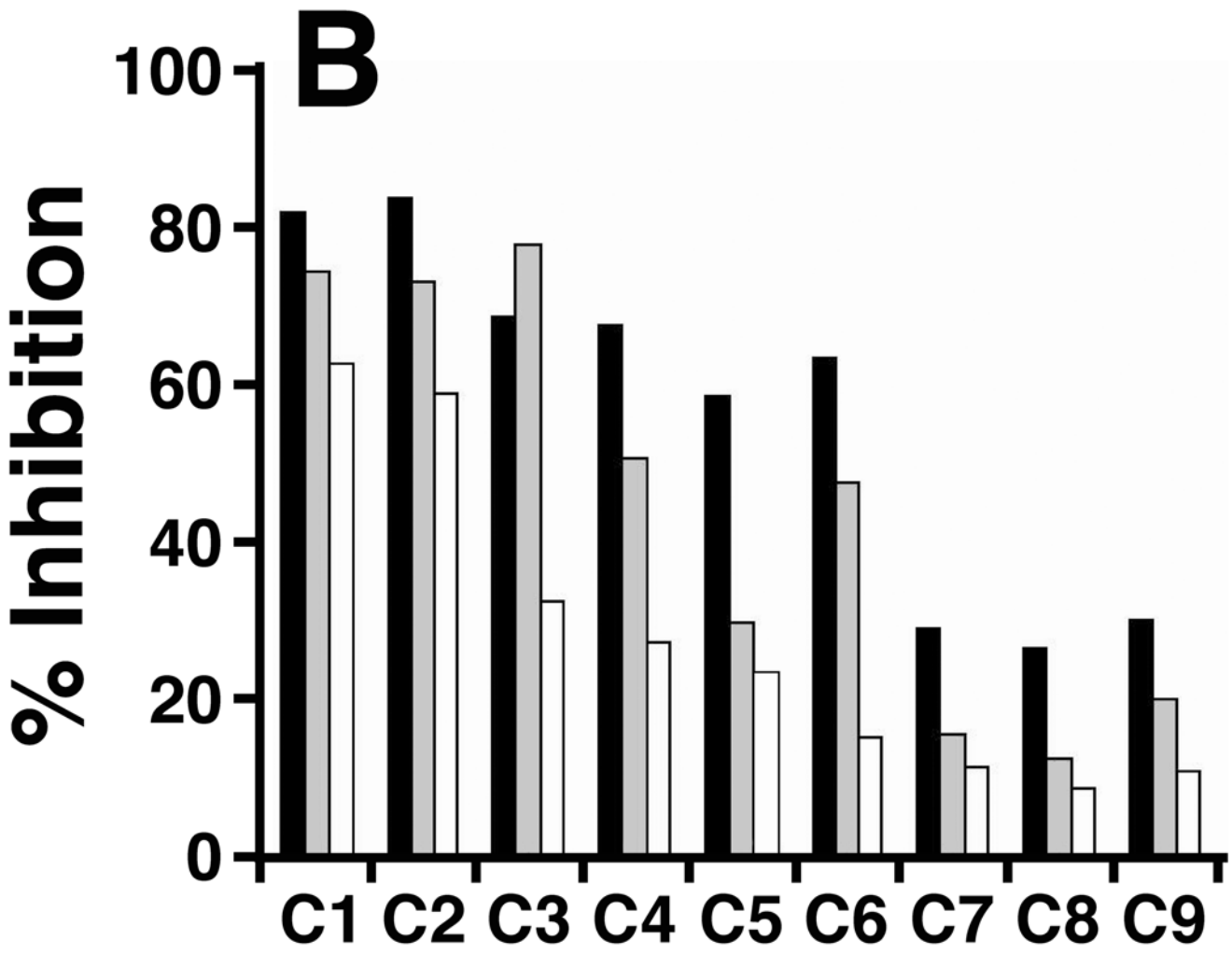
B
100
80
60
40
20
0
% Inhibition
C1 C2 C3 C4 C5 C6 C7 C8 C9

Fig. 1

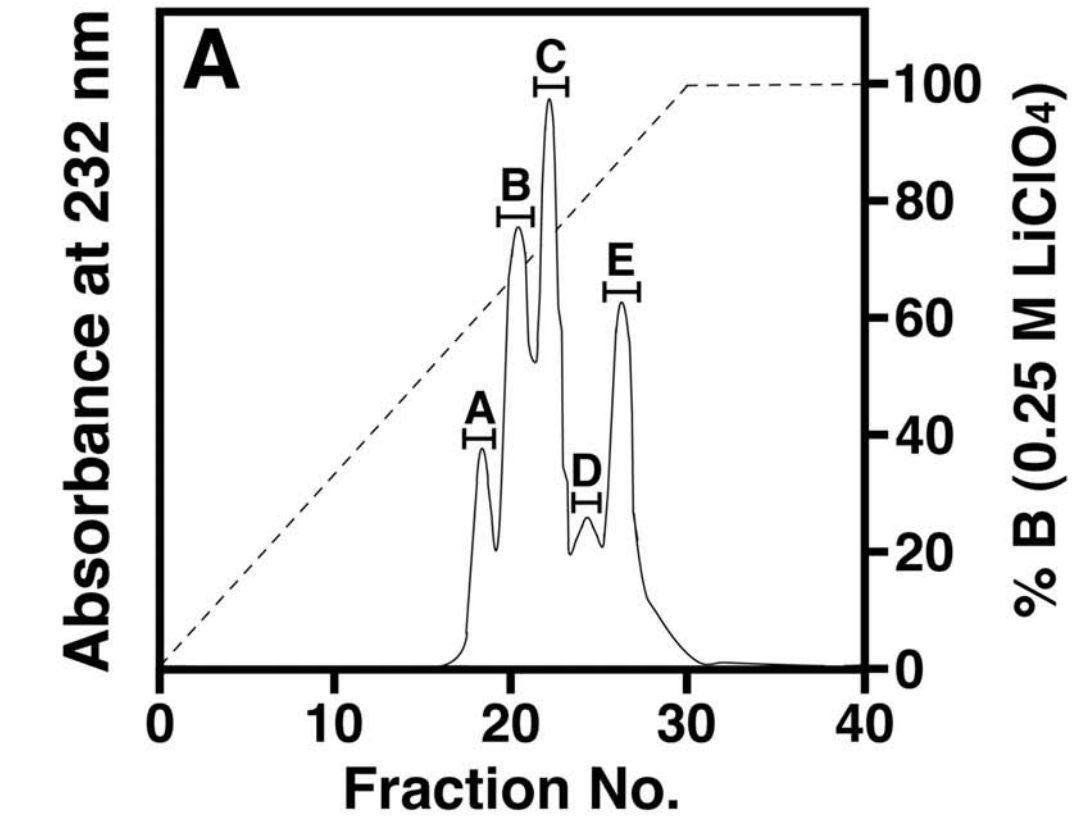
A
Absorbance at 232 nm
% B (0.25 M LiClO4)
Fraction No.
A
B
C
D
E
0
10
20
30
40
0
20
40
60
80
100

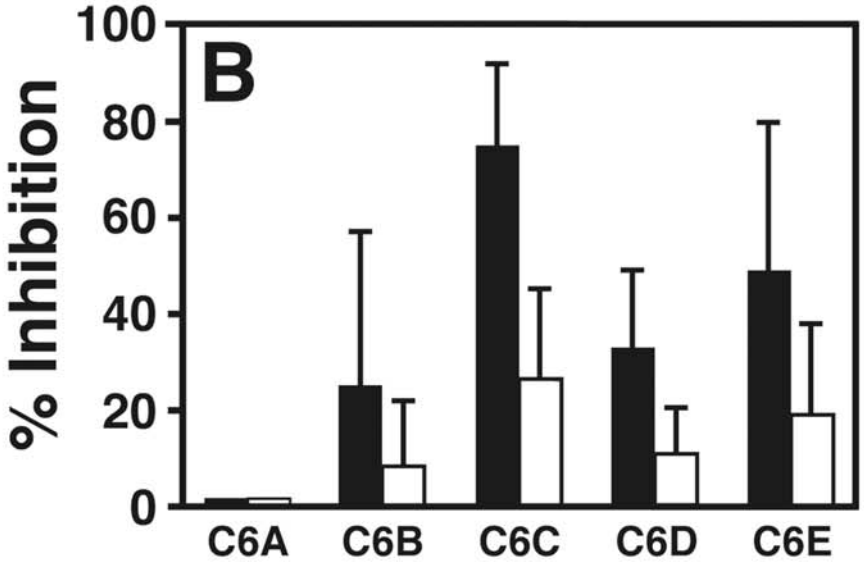
B
% Inhibition
0
20
40
60
80
100
C6A
C6B
C6C
C6D
C6E

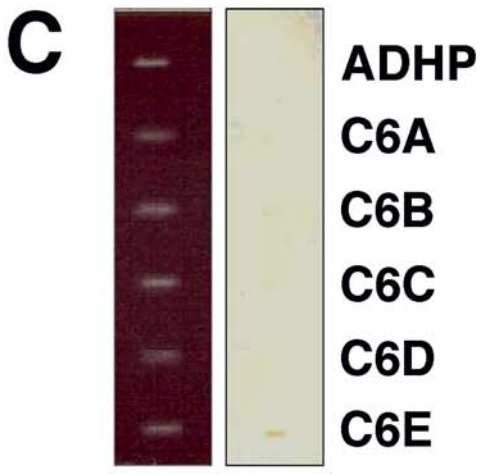
C
ADHP
C6A
C6B
C6C
C6D
C6E

Fig.2

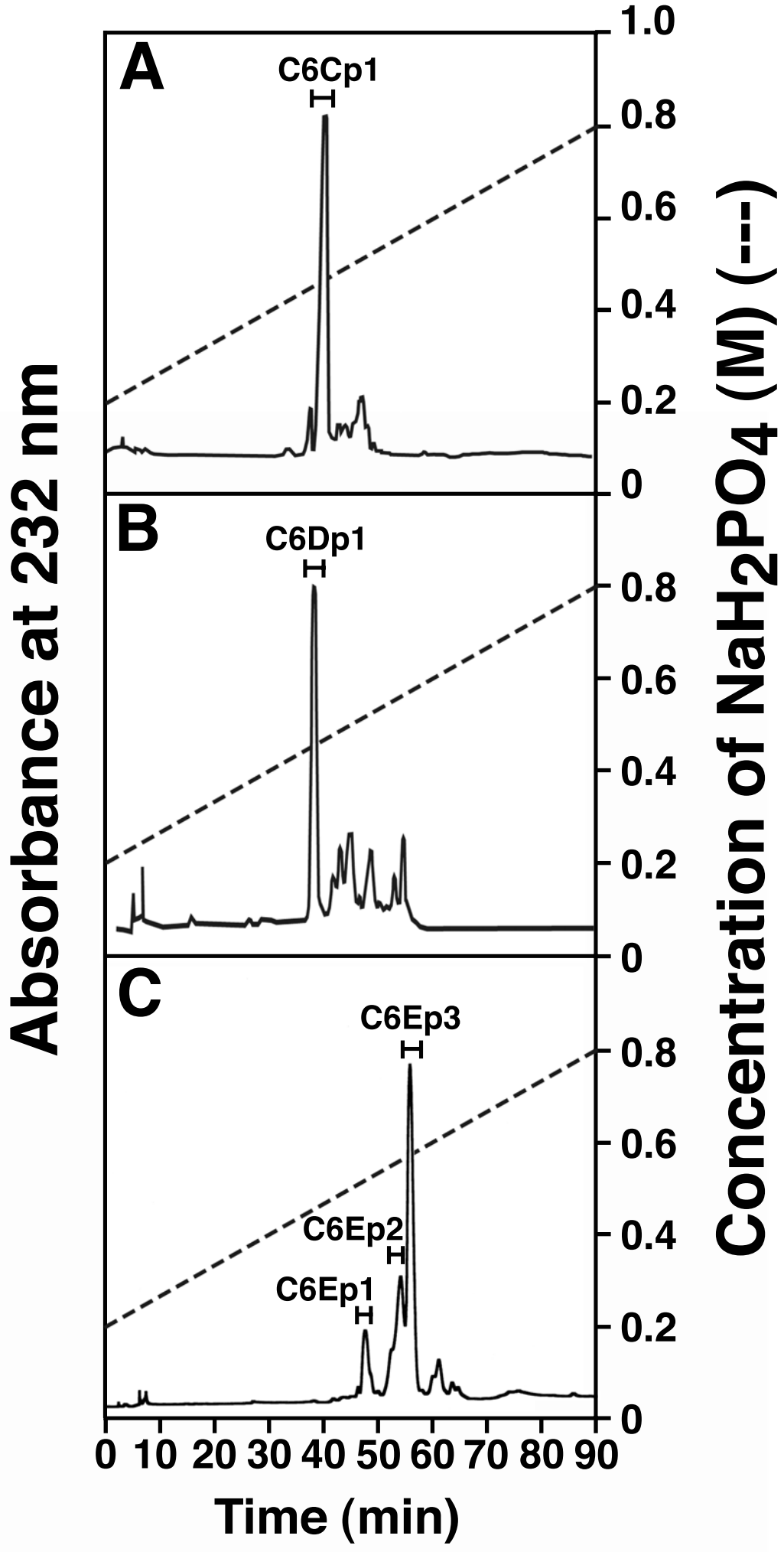
A
C6Cp1
B
C6Dp1
C
C6Ep3
C6Ep2
C6Ep1
1.0
0.8
0.6
0.4
0.2
0
0 10 20 30 40 50 60 70 80 90
Time (min)
Absorbance at 232 nm
Concentration of NaH2PO4 (M) (---)

Fig. 3

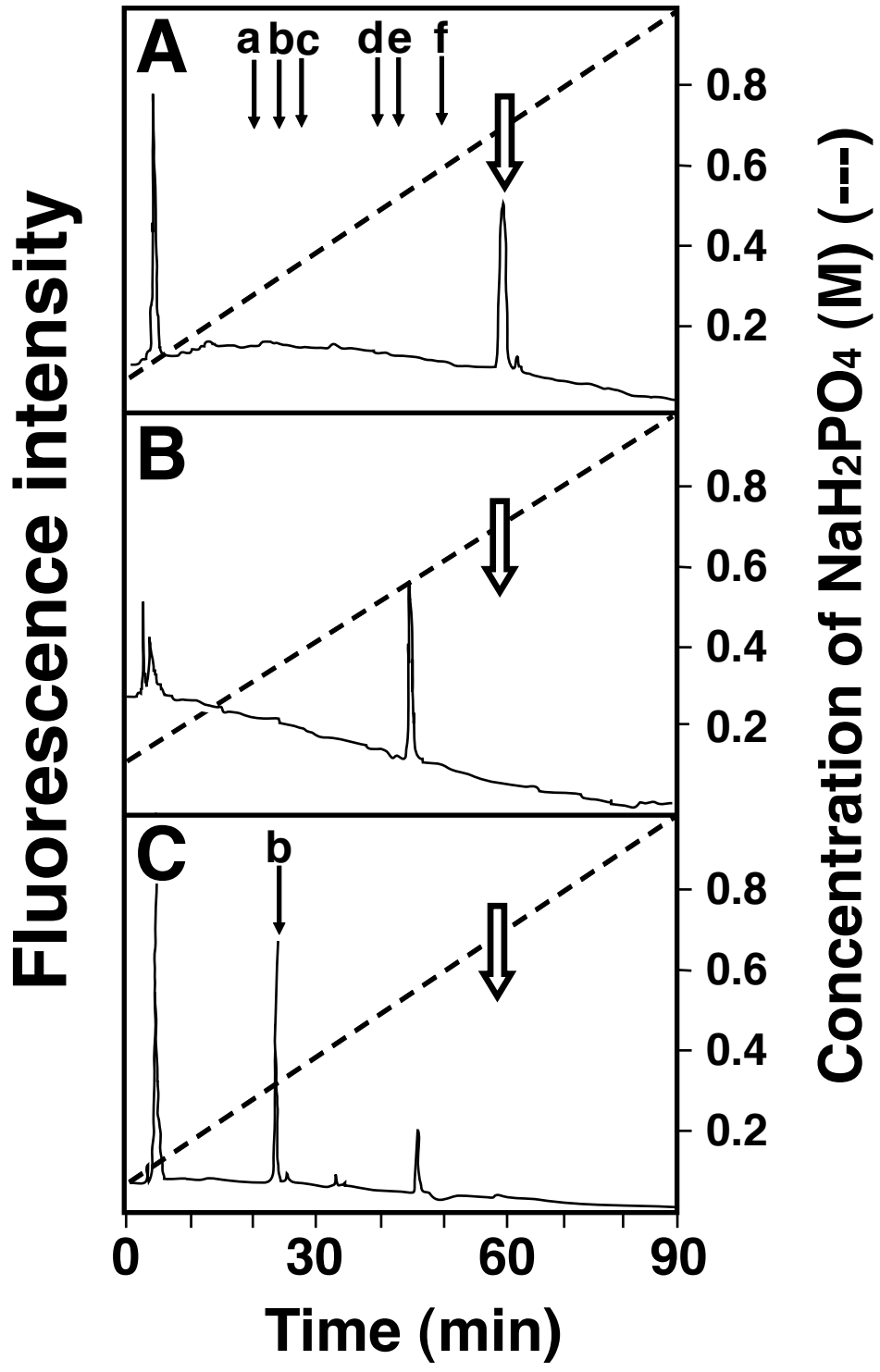
A
a b c d e f
B
C
b
0.8
0.6
0.4
0.2
0
30
60
90
Time (min)
Fluorescence intensity
Concentration of NaH2PO4 (M) (---)

Fig. 4

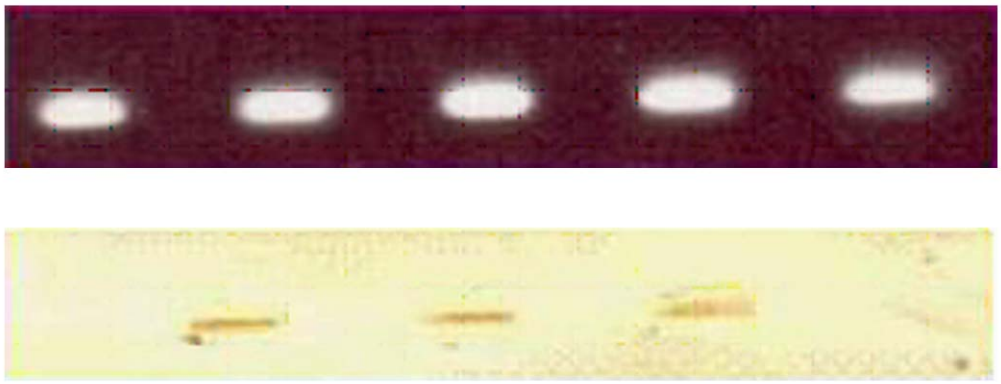

ADHP C6Ep1 (ΔDCCC) C6Ep2 (ΔCCAD) Standard (CCAD) C6Ep3 (ΔCADC)

Fig. 5

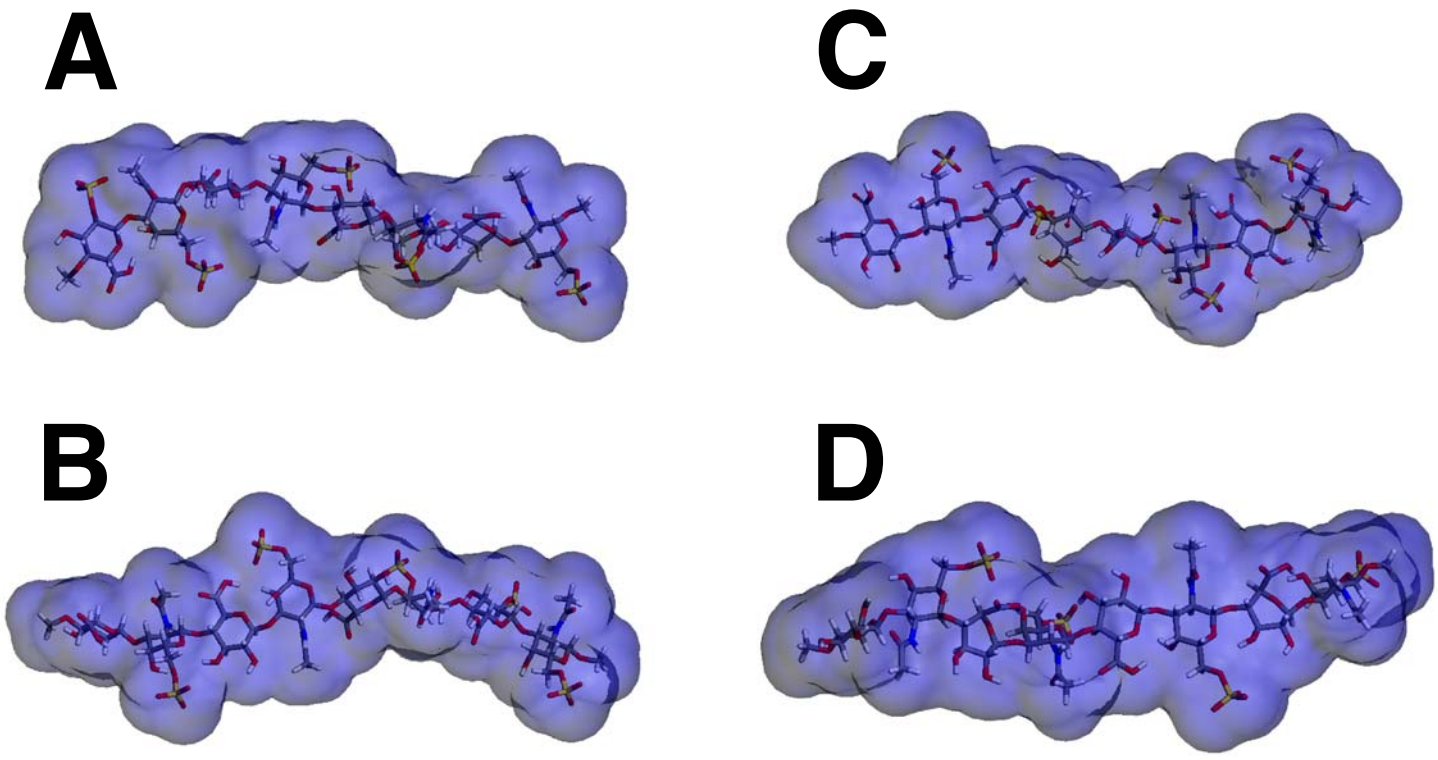

Fig. 6

A

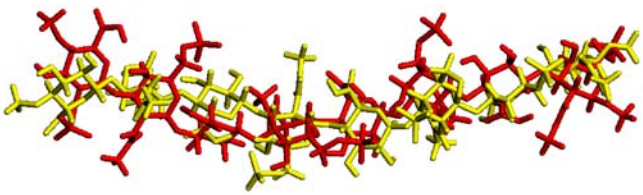

RMSD: 4.898Å

D

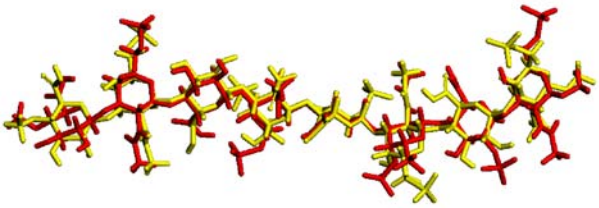

RMSD: 0.369Å

B

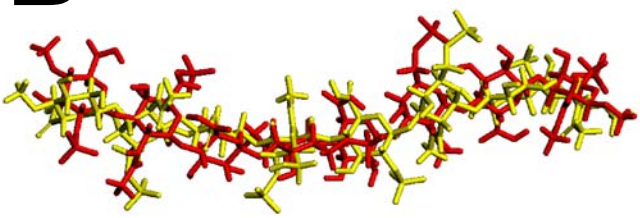

RMSD: 4.929Å

E

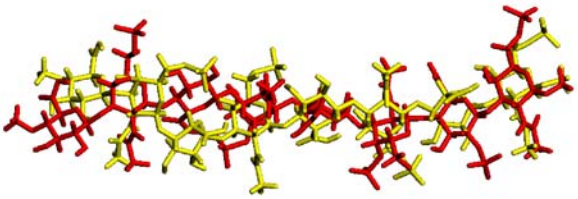

RMSD: 6.693Å

C

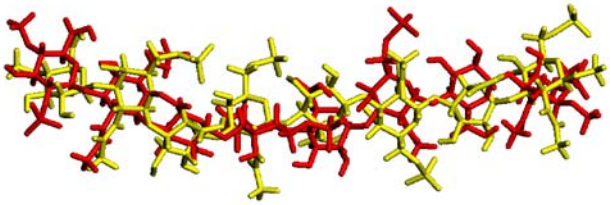

RMSD: 4.033Å

Fig. 7

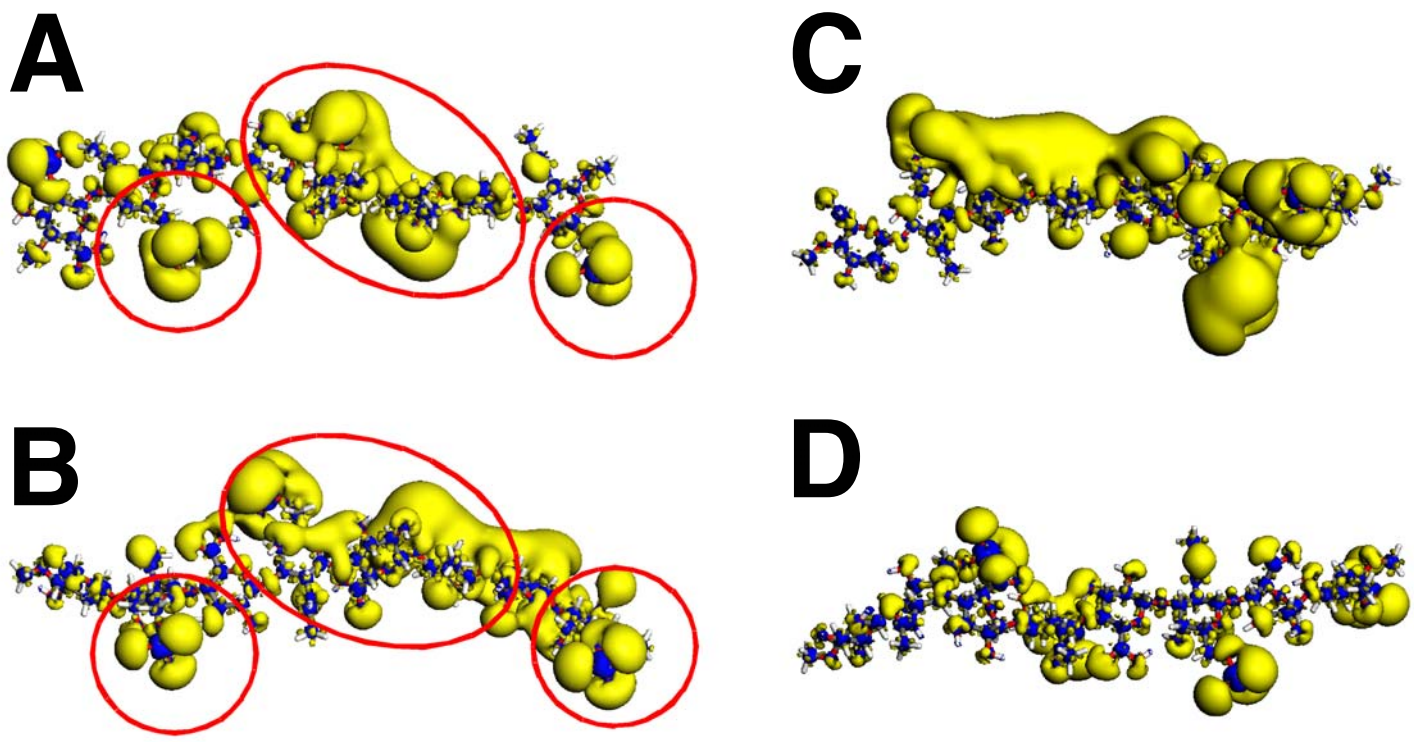

Fig. 8

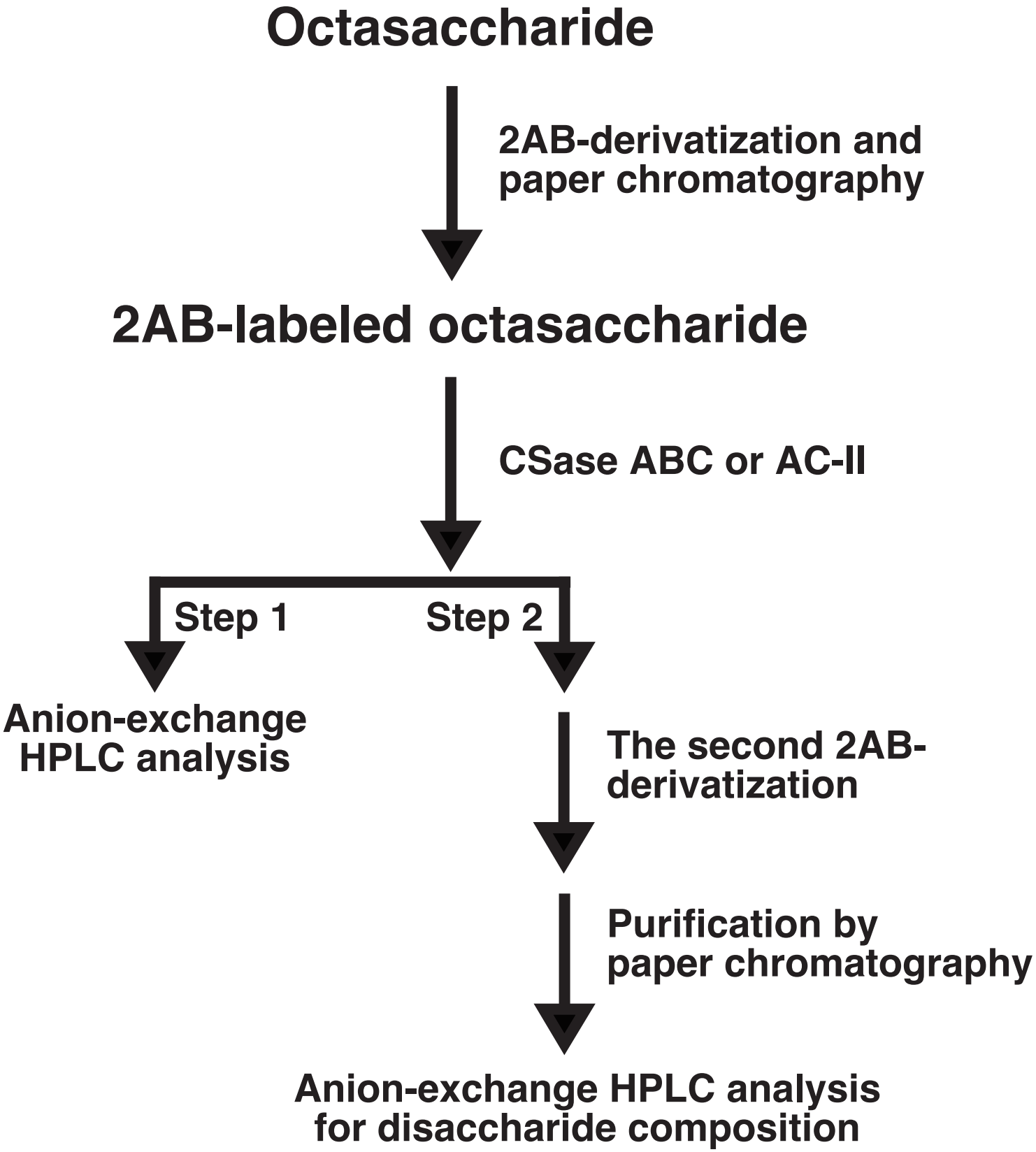
Octasaccharide
2AB-derivatization and paper chromatography
2AB-labeled octasaccharide
CSase ABC or AC-II
Step 1
Step 2
Anion-exchange HPLC analysis
The second 2AB-derivatization
Purification by paper chromatography
Anion-exchange HPLC analysis for disaccharide composition

Scheme 1

Supplemental Table S1

Twenty-four initial conformations were chosen for each CS disaccharide in the range of (40°-330°, 60°-330°) and then the full geometry optimizations were performed using the semi-empirical molecular orbital calculations taking the solvent effects into accounts. Optimized dihedral angles (ϕ, ψ) of the CS disaccharides in the local energy minima are summarized and the values in bold have been used for Table VIA. FE stands for the formation energy. The (ϕ, ψ) values of the disaccharide subunits in the four octasaccharides were also determined by the full geometry optimizations, and are summarized in the bottom half of Supplemental Table S1, which have been taken from Table VIB for comparison with the (ϕ, ψ) values obtained for the individual CS disaccharides.

CS disaccharides	GlcUA-GalNAc(6S)			GlcUA-GalNAc(4S)			GlcUA(2S)-GalNAc(6S)			GalNAc(6S)-GlcUA			GalNAc(4S)-GlcUA(2S)		
initial (ϕ, ψ)	ϕ	ψ	FE/kcal/mol	ϕ	ψ	FE/kcal/mol	ϕ	ψ	FE/kcal/mol	ϕ	ψ	FE/kcal/mol	ϕ	ψ	FE/kcal/mol
(330, 100)	282	78	-845.6	284	106	-838.2	**295**	**114**	**-1102.1**	301	96	-840.3	301	242	-1093.1
(290, 100)	283	79	-845.6	284	106	-838.2	279	82	-1098.8	301	92	-841.7	290	260	-1093.5
(244, 100)	282	78	-846.1	257	91	-835.2	279	82	-1098.6	301	92	-841.7	279	232	-1091.2
(180, 100)	281	78	-846.4	192	70	-835.0	284	83	-1096.7	268	62	-839.8	221	213	-1093.9
(130, 100)	67	98	-843.8	65	100	-836.1	91	127	-1087.1	291	265	-843.6	**53**	**236**	**-1096.2**
(80, 100)	69	98	-843.3	67	99	-835.7	76	104	-1097.5	22	189	-845.0	273	295	-1091.0
(40, 100)	281	78	-845.4	65	99	-835.8	57	105	-1097.3	**62**	**89**	**-836.7**	51	237	-1095.2
(290, 60)	282	78	-846.2	282	105	-838.2	278	79	-1098.9	**301**	**92**	**-845.6**	297	271	-1092.9
(290, 140)	**281**	**77**	**-846.6**	286	109	-837.3	277	80	-1099.3	301	94	-840.8	**254**	**214**	**-1094.3**
(290, 180)	282	78	-845.6	287	109	-837.4	278	81	-1099.4	246	195	-841.6	264	163	-1090.4
(290, 230)	**279**	**262**	**-845.4**	**274**	**289**	**-837.6**	**260**	**282**	**-1099.2**	311	239	-841.6	305	92	-1092.2
(290, 280)	250	286	-841.3	269	291	-835.6	260	281	-1097.4	309	239	-841.7	304	93	-1091.4
(290, 330)	260	290	-841.4	268	290	-836.4	271	294	-1098.9	**301**	**241**	**-846.2**	272	59	-1089.8
(80, 60)	**70**	**99**	**-846.3**	67	98	-834.3	40	108	-1098.0	64	86	-836.5	78	263	-1092.7
(80, 140)	62	94	-842.3	65	100	-835.8	**69**	**109**	**-1099.4**	15	204	-842.2	51	238	-1095.1
(80, 180)	97	139	-839.9	**93**	**147**	**-838.7**	89	131	-1095.6	15	197	-844.0	50	238	-1095.6
(80, 230)	327	295	-840.4	95	137	-835.2	80	161	-1092.0	49	238	-843.5	296	241	-1092.5
(80, 280)	68	310	-838.6	**86**	**302**	**-826.9**	313	70	-1091.8	70	282	-840.0	60	86	-1088.9
(80, 330)	70	310	-837.4	**276**	**127**	**-838.3**	**68**	**315**	**-1095.1**	**50**	**238**	**-846.5**	**58**	**79**	**-1093.3**
(330, 280)	282	307	-843.8	268	290	-837.5	283	306	-1098.9	309	240	-841.5	304	93	-1095.1
(235, 280)	259	279	-842.3	269	291	-837.0	283	306	-1099.1	248	196	-843.3	265	60	-1090.4
(180, 280)	258	279	-842.1	266	288	-837.2	253	212	-1087.8	248	195	-843.8	**303**	**94**	**-1097.8**
(130, 280)	**72**	**310**	**-839.3**	84	303	-825.3	61	325	-1087.5	50	237	-845.2	61	89	-1089.5
(40, 280)	297	325	-839.5	301	311	-831.1	22	277	-1090.2	49	238	-843.9	59	85	-1089.6
ΔCADC-21	272	129	-			-			-			-			-
ΔCCAD-65	284	98	-			-			-			-			-
ΔCCCC-65	274	139	-			-			-			-			-
ΔCCCC-43	276	77	-			-			-			-			-
ΔCCCC-21	257	60	-			-			-			-			-
ΔDCCC-65	274	139	-			-			-			-			-
ΔDCCC-43	292	86	-			-			-			-			-
ΔDCCC-21	312	155	-			-			-			-			-
ΔCADC-65			-	292	107	-			-			-			-
ΔCCAD-43			-	281	126	-			-			-			-
ΔCADC-43			-			-	292	130	-			-			-
ΔCCAD-21			-			-	279	94	-			-			-
ΔCADC-76			-			-			-	283	244	-			-
ΔCADC-32			-			-			-	282	249	-			-
ΔCCAD-76			-			-			-	298	243	-			-
ΔCCAD-54			-			-			-	282	247	-			-
ΔCCCC-76			-			-			-	260	56	-			-
ΔCCCC-54			-			-			-	304	240	-			-
ΔCCCC-32			-			-			-	272	208	-			-
ΔDCCC-76			-			-			-	288	90	-			-
ΔDCCC-54			-			-			-	311	267	-			-
ΔDCCC-32			-			-			-	265	207	-			-
ΔCADC-54			-			-			-			-	296	246	-
ΔCCAD-32			-			-			-			-	299	236	-